

AD 675500

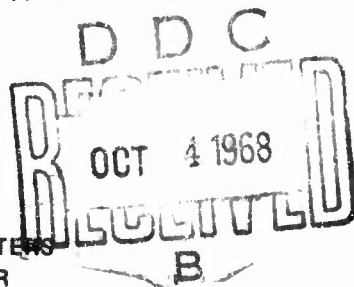
# PROJECT SQUID

## TECHNICAL REPORT CAL-96-PU

### RELAXATION IN GAS-PARTICLE FLOW

By  
GEORGE RUDINGER  
Cornell Aeronautical Laboratory, Inc.  
Buffalo, New York

PROJECT SQUID HEADQUARTERS  
JET PROPULSION CENTER  
SCHOOL OF MECHANICAL ENGINEERING  
PURDUE UNIVERSITY  
LAFAYETTE, INDIANA



Project SQUID is a cooperative program of basic research relating to Jet Propulsion. It is sponsored by the Office of Naval Research and is administered by Purdue University through Contract N00014-67-A-0226-0005, NR-098-038.

JULY 1968

This document has been approved  
for public release and sale; its  
distribution is unlimited

Reprinted by the  
CLEARINGHOUSE  
for Federal Scientific & Technical  
Information Springfield, Va. 22151

Project SQUID Technical Report No. CAL-96-PU

RELAXATION IN GAS-PARTICLE FLOW \*+

by

George Rudinger  
Cornell Aeronautical Laboratory, Inc.  
Buffalo, New York

July 1968

- 
- \* This work was sponsored by Project SQUID which is supported by the Office of Naval Research, Department of the Navy, under Contract N00014-67-A-0226-0005, NR-098-038. Reproduction in full or in part is permitted for any use of the United States Government.
  - + This paper was prepared as a chapter for a forthcoming book on Nonequilibrium Flow (P. P. Wegener, Editor) to be published by Marcel Dekker, Inc., New York.

## SUMMARY

Flow of gas-particle mixtures may exhibit significant relaxation effects if the particle velocity and temperature cannot follow rapid changes in the flow conditions. These relaxation phenomena are first demonstrated in a discussion of viscous drag and heat transfer for a single particle which has no effect on the gas flow. If there are enough particles to make up a significant fraction of the mass of the mixture, the thermodynamic properties of the mixture may differ considerably from those of the gas alone, and a number of these properties are derived. Equations for one-dimensional flow of uniform mixtures are applied to shock waves, steady nozzle flows, and general nonsteady flows to illustrate the relaxation processes. For low and moderate particle concentrations, the volume occupied by the particles can often be neglected. Since this assumption may not be adequate for high concentrations, some effects of a finite particle volume are also discussed.

# RELAXATION IN GAS-PARTICLE FLOW \*

George Rudinger

Cornell Aeronautical Laboratory, Inc.

Buffalo, New York

## Contents

1. Introduction
2. Gas-Particle Interaction for Single Particles
  - a) Viscous Drag
  - b) Heat Transfer
3. Thermodynamic Properties of Gas-Particle Mixtures
4. General Equations for One-Dimensional Gas-Particle Flow
5. Shock Waves
  - a) Discontinuous Shock Front
  - b) Dispersed Shock Waves
6. Nozzle Flow
7. Nonsteady Flow
8. Concluding Remarks
9. List of Symbols
10. References

---

\* This work was sponsored by Project SQUID which is supported by the Office of Naval Research, Department of the Navy, under Contract N00014-67-A-0226-0005, NR-098-038. Reproduction in full or in part is permitted for any use of the United States Government.

## 1. INTRODUCTION

There are many engineering applications for flows of a medium that consists of a suspension of powdered material or liquid droplets in a gas. A typical example is the flow in rockets that use a solid propellant to which aluminum powder has been added for the purpose of improved flame stability and heat release. As a result, small solid particles of aluminum oxide are formed which must be exhausted with the rest of the combustion gases. Other examples occur in connection with some nuclear reactors, fuel sprays, air pollution and conveying of powdered materials.

Most of these flows involve changes of the gas velocity and temperature. Gas-particle interaction through viscous drag and heat transfer produces corresponding changes in the particles. These processes are relatively slow, so that for fast changes in the gas phase, considerable deviations from equilibrium may occur. Thus, one has to deal with typical relaxation processes.

A flow of a pure gas with sufficiently large and rapid temperature changes deviates from thermodynamic equilibrium because some degrees of freedom in the molecules cannot follow these changes without lag. This behavior has led to such concepts as translational and vibrational temperatures. Similarly, a gas-particle flow must be characterized by a gas temperature and a possibly different particle temperature. Further complications arise because the velocity of the particles also may be different from that of the gas.

A single particle that is not in equilibrium with the gas flow simply represents a poor "tracer," but if there are enough particles to form a significant fraction of the mass of the mixture, their interaction with the gas affects the gas flow. Rather complicated flows can therefore develop as a result of the relaxation processes. As in the case of pure gas flows, the rate at which deviations from equilibrium tend to be eliminated may be fast or slow compared with the rate at which flow changes take place. It is therefore possible to consider "frozen" flow in which no relaxation processes take place, equilibrium flows for which relaxation is assumed to be infinitely fast, and intermediate nonequilibrium flows.

Only momentum exchange and heat transfer between the gas and the particles has been mentioned so far. Mass transfer by condensation, evaporation, or chemical reaction represents another important process, but only permanent particles will be considered here. No distinction will be made between solid particles and liquid droplets. \* All flows will be treated as one-dimensional, that is, the particles will be assumed to be uniformly distributed over the cross section of a duct. There are many important situations in which the particle distribution is not uniform or the flow not one-dimensional. These involve considerable complications of the analysis without contributing to further insight into the relaxation processes and therefore will not be considered.

---

\* When the gas velocity differs sufficiently from that of a liquid droplet, the latter may break up as a result of the shear force (Gordon, 1959). This phenomenon also will not be considered.

The discussion starts with a description of the nature of gas-particle interactions and the behavior of single particles. Before considering flows of gas-particle mixtures, the thermodynamic properties of such mixtures will be derived, since they may differ considerably from those of the gas alone. The equations which describe one-dimensional flow then are derived and applied to several typical cases to illustrate various aspects of the flow modifications that result from the presence of the particles.

Frequent references to previous publications are given; most of these should be considered as representative examples, and no attempt is made to provide a complete bibliography. Extensive analytical studies that are published elsewhere are outlined only in general. Reference to the original literature should be made for further details.

## 2. GAS PARTICLE INTERACTION

### a. Viscous Drag

Before discussing flows of gas-particle mixtures, it is helpful to consider the behavior of a single particle that is not in equilibrium with the surrounding gas and does not affect the gas except in its immediate vicinity. Important qualitative aspects of the relaxation processes can be brought out by this approach.

Consider a spherical particle of diameter  $D$  and density  $\rho_p$  moving with a velocity  $u_p$  in a gas having a density  $\rho$  and velocity  $u$  that need not be constant. In the absence of external forces and for sufficiently small relative velocities, the equation of motion is given by (Hinze, 1959)

$$\begin{aligned} \frac{\pi D^3}{6} \rho_p \frac{D_p u_p}{Dt} = & 3\pi\mu D (u - u_p) - \frac{\pi D^3}{6} \frac{\partial p}{\partial x} \\ & + \frac{1}{2} \frac{\pi D^3}{6} \rho \left( \frac{Du}{Dt} - \frac{D_p u_p}{Dt} \right) + \frac{3}{2} D^2 \sqrt{\pi \rho \mu} \int_0^t \frac{\frac{Du}{Dt'} - \frac{D_p u_p}{Dt'}}{\sqrt{t-t'}} dt' \end{aligned} \quad (2.1)$$

where  $\mu$  is the viscosity of the gas, and  $x$  and  $t$  are the position and time coordinates. The substantial derivatives must be taken along the trajectories of the gas and of the particles, so that

$$\frac{D}{Dt} = \frac{\partial}{\partial t} + u \frac{\partial}{\partial x} \quad \text{and} \quad \frac{D_p}{Dt} = \frac{\partial}{\partial t} + u_p \frac{\partial}{\partial x} \quad (2.2)$$

The left-hand side of Eq. (2.1) represents the product of particle mass and acceleration. The right-hand side indicates the various forces that act on the particle, and the first term is the viscous drag according to Stokes' law. The second term represents the effect of the pressure gradient in the gas which may be expressed by the acceleration of the gas according to the momentum equation (Hinze, 1959)

$$\rho \frac{Du}{Dt} = - \frac{\partial p}{\partial x} \quad (2.3)$$

In gas-particle flows, Eq. (2.3) does not hold (see Section 4), and this substitution is then not permissible. The third term indicates the force needed to accelerate the added mass of the particle relative to the fluid (for spherical particles, the added mass is equal to one-half of the mass of the displaced fluid), and the integral term accounts for the deviations

of the flow pattern around the particle from that for steady flow. Under the usual conditions in which  $\rho_p$  exceeds  $\rho$  by about three orders of magnitude, only the viscous drag needs to be considered and the other terms may be neglected (Hinze, 1959; Fuchs, 1964, pp. 70-73). This simplification may not be permissible under unusual conditions (high gas pressures or hollow particles), but such situations will not be considered.

If the particle velocity with respect to the gas is large enough, Stokes drag in Eq. (2.1) becomes inaccurate, and a more appropriate drag force should be used. This force is expressed as the product of the dynamic head of the relative motion acting on the cross-sectional area of the particle and an empirical drag coefficient  $C_D$ , so that

$$\text{Drag} = C_D \frac{\pi D^2}{4} \frac{1}{2} \rho |u - u_p| (u - u_p) \quad (2.4)$$

Writing the square of the relative velocity in this form insures that the drag always has the correct sign. After substituting Eq. (2.4) for the viscous-drag term in Eq. (2.1), omitting the negligible terms, and dividing by the mass of the particle, the equation of motion for a single solid particle in a gas becomes

$$\frac{D_p u_p}{Dt} = C_D \frac{3}{4D} \frac{\rho}{\rho_p} |u - u_p| (u - u_p) \quad (2.5)$$

In general, the drag coefficient is expressed as an empirical function of the particle Reynolds number which always is taken as a positive quantity

$$Re = \frac{\rho D |u - u_p|}{\mu} \quad (2.6)$$

Stokes drag corresponds to

$$C_D = \frac{24}{Re} \quad (2.7a)$$

Although Eq. (2.7a) is valid only for small Reynolds numbers ( $Re < 1$ ), it is often used for qualitative studies because it leads to the simple expression shown in Eq. (2.1). For larger Reynolds numbers, extensive experimental determinations of the drag coefficient have been made (Schlichting, 1955, or Fuchs, 1964, p. 32). These results will be referred to as the "standard" drag coefficient for want of a generally accepted name. They are shown in Fig. 1 for Reynolds numbers below one thousand which are of interest for gas-particle flows. Various analytical approximations to this relationship may be found in the literature. For example, Gilbert, Davis and Altman (1955) used

$$C_D = 0.48 + \frac{28}{Re^{0.85}} \quad (2.7b)$$

and Kliachko (Fuchs, 1964, p. 33) suggested

$$C_D = \frac{24}{Re} + \frac{4}{Re^{1/3}} \quad (2.7c)$$

(The reciprocal of the first term in this reference is an obvious misprint.)

The latter formula approaches Stokes drag for small Reynolds numbers and should also be convenient for analytical studies (Putnam, 1961), but apparently it has not been used extensively. Other expressions for the

drag coefficient may be used for gas-particle flows as discussed in Section 4. A few points, representing Eqs. (2.7b) and (2.7c) are entered in Fig. 1 to demonstrate that these equations give a good fit to the standard drag coefficient in the range of interest, while the Stokes drag of Eq. (2.7a) is markedly too low for higher Reynolds numbers.

In the foregoing discussion, continuum flow around the particle is implied, that is, the molecular mean free path in the gas must be small compared with the particle dimensions. For particles much smaller than one micron, this condition is usually not satisfied, and corrections to the drag coefficient must be applied. Such corrections may be found in the literature (Schaaf and Chambre, 1958; Carlson and Hoglund, 1964; Willis, 1966; and Crowe, 1967), but their inclusion in the analysis would go beyond the scope of the present discussion.

Consider the motion of a single particle in a gas that flows with a constant velocity  $u$ , and assume that Stokes drag can be applied. Equation (2.5) then becomes

$$\frac{du_p}{dt} = \frac{18\mu}{D^2\rho_p} (u - u_p) \quad (2.8)$$

with the solution

$$u_p - u = (u_{p,0} - u) e^{-t/\tau_v} \quad (2.9)$$

where  $u_{p,0}$  is the initial particle velocity, and

$$\tau_v = \frac{D^2 \rho_p}{18 \mu} \quad (2.10)$$

is the relaxation time for the particle velocity. The distance by which a particle slips with respect to the gas before reaching equilibrium is readily obtained by integration of Eq. (2.9) from zero to infinity with the result that the slip is equal to  $\tau_v (u_p - u)$ .

If the drag coefficient were given by another expression, the resultant differential equation would, in general, have to be solved numerically (for instance, Hoenig, 1957), and the result would no longer be a simple exponential function. Nevertheless,  $\tau_v$  would still be a convenient qualitative measure of velocity relaxation and would also be a natural reference time for dimensionless representation of data.

#### b. Heat Transfer

Temperature relaxation of a particle may be treated similarly to velocity relaxation. Let  $T$  and  $T_p$  be the gas and the particle temperatures and  $h$  the heat-transfer coefficient. The heat balance for a spherical particle then becomes

$$\frac{\pi D^3}{6} \rho_p c \frac{dT_p}{dt} = h \pi D^2 (T - T_p) \quad (2.11)$$

where  $c$  is the specific heat of the particle material. The heat-transfer coefficient is conveniently expressed in terms of a Nusselt number

$$Nu = \frac{hD}{k} \quad (2.12)$$

where  $k$  is the thermal conductivity of the gas. For pure heat conduction, a value  $Nu = 2$  applies, but if the particle moves with respect to the gas, additional heat transfer by convection takes place. The Nusselt number then may be expressed as a function of the particle Reynolds number, and several such relationships can be found in the literature. One frequently used empirical relationship for steady flow is (Knudsen and Katz, 1958)

$$Nu = 2 + 0.6 Pr^{1/3} Re^{1/2} \quad (2.13)$$

where  $Pr = \mu c_p / k$  is the Prandtl number, and  $c_p$  the specific heat of the gas at constant pressure. This relationship is shown in Fig. 2 for  $Pr = 0.7$ , which is a reasonable value for many commonly used gases. If the particle temperature were high enough for radiative heat transfer to become important, a more elaborate heat-transfer coefficient would be needed (Simmons and Spadaro, 1965). As in the case of the drag coefficient, a correction should be applied if the assumption of continuum flow around the particle does not hold (Schaaf and Chambré, 1958), but only continuum flow will be considered in the following.

If  $Nu = 2$  is assumed, Eqs. (2.11) and (2.12) are easily solved for a constant gas temperature with the result

$$T_p - T = (T_{p,0} - T) e^{-t/\tau_T} \quad (2.14)$$

where  $T_{p,0}$  is the initial particle temperature and

$$\tau_T = \frac{1}{12} \frac{D_p^2 c_p \rho}{k} = \frac{3}{2} Pr \frac{5}{4} \tau_v \quad (2.15)$$

is the relaxation time for heat transfer. The relationship between  $\tau_T$  and  $\tau_v$  is established through Eq. (2.10), where the ratio  $\xi = c/c_p$  has been introduced. Since the Prandtl number of many gases is close to 2/3 and  $\xi$  is of order unity for many gas-particle combinations, it can be seen that the temperature and velocity relaxation times are approximately equal (Marble, 1963a). If the Reynolds number term in Eq. (2.13) cannot be neglected, Eq. (2.11) must be integrated numerically and  $\tau_T$  is then only a convenient qualitative measure of temperature relaxation.

In the foregoing discussion it was assumed that the temperature is uniform inside the particle, but heat flow into, or out of, a particle leads to internal temperature gradients. The question arises therefore, whether heat conduction within the particle reduces these gradients fast enough that a single temperature can be assigned to the particle. To evaluate this process, assume that the surface temperature is suddenly changed and maintained at a new level. Let  $q_\infty$  be the total amount of heat that must be transferred to reestablish equilibrium, and  $q$  the heat transferred after a time  $t$ . The ratio  $q/q_\infty$  is given by (Carslaw and Jaeger, 1959) as

$$\frac{q}{q_\infty} = 1 - \frac{6}{\pi} \sum_{n=1}^{\infty} \frac{1}{n^2} e^{-n^2 \pi^2 \theta} \quad (2.16)$$

where  $\theta = 4 \kappa_p t / D^2$  is a dimensionless time and  $\kappa_p$  is the thermal diffusivity of the particle material. Evaluation of Eq. (2.16) yields the following values

$\theta = 4\kappa_p t/D^2$	0.1	0.2	0.4	0.6	0.8
$q/q_\infty$	0.7705	0.9155	0.9883	0.9984	0.9998

These show that almost 99% of the heat transfer is completed when  $\theta = 0.4$  or when  $t = 0.1 D^2 / \kappa_p = \tau_i$ . The time  $\tau_i$  thus may be considered as a measure for the rate of internal temperature equalization and compared with the relaxation time for heat transfer  $\tau_r$ . From the definition  $\kappa_p = k_p / \rho_p c$ , where  $k_p$  is the thermal conductivity of the particle material, and Eq. (2.15) the ratio  $\tau_i / \tau_r$  is found to be approximately equal to the ratio of the thermal conductivities  $k/k_p$ . For metallic particles in air, this ratio is of the order of only  $10^{-4}$ , and for most insulating materials in air it is still less than 0.1. For extreme conditions, however, the ratio may approach unity and even exceed this value. For example, it reaches a value of about two for magnesium oxide in hydrogen. Effects of such long temperature equalization times on gas-particle flows apparently have not yet been studied. As demonstrated by the examples in Section 5, an error in the assumed heat transfer may not affect particle motion significantly.

### 3. THERMODYNAMIC PROPERTIES OF GAS-PARTICLE MIXTURES

In describing the thermodynamic properties of a gas-particle mixture, a careful distinction must be made between the density of the particle material  $\rho_p$  and the amount of particle material in a unit volume of the mixture (Rudinger, 1965). The latter quantity will be denoted by  $\sigma_p$  and

might be called the particle concentration. Similarly, there is a distinction between the gas density  $\rho$  and the gas concentration  $\sigma$ . If  $\epsilon$  denotes the volume fraction of the particles, then, clearly, one has

$$\sigma_p = \epsilon \rho_p \quad \text{and} \quad \sigma = (1 - \epsilon) \rho \quad (3.1)$$

The mass fraction of the particles  $\Phi$  is given by

$$\Phi = \frac{\sigma_p}{\sigma + \sigma_p} \quad (3.2)$$

Combination of these relationships yields

$$\frac{\epsilon}{1 - \epsilon} = \frac{\sigma_p}{\sigma} \frac{\rho}{\rho_p} = \frac{\Phi}{1 - \Phi} \frac{\rho}{\rho_p} \quad (3.3)$$

and

$$\sigma = \rho \left( 1 - \frac{\sigma_p}{\rho_p} \right) \quad (3.4)$$

If the mixture is flowing through a duct of cross section  $A$ , the local mass flow rates of the gas and of the particles are given by  $\dot{m} = \sigma u A$  and  $\dot{m}_p = \sigma_p u_p A$ . These flow rates are constant only if the flow is steady. Let the mass-flow ratio (loading ratio) be denoted by  $\eta$  so that

$$\eta = \frac{\sigma_p u_p}{\sigma u} = \frac{\epsilon}{1 - \epsilon} \frac{\rho_p}{\rho} \frac{u_p}{u} = \frac{\Phi}{1 - \Phi} \frac{u_p}{u} \quad (3.5)$$

This equation shows clearly that, although  $\eta$  is constant for a steady flow,  $\Phi$  is constant only if the ratio  $u_p/u$  is also constant.

In contrast,  $\epsilon$  is constant only if  $\sigma_p$  is constant, because the particles may be considered as incompressible. It is evident from Eq. (3.3) that, under the usual conditions for which the density ratio  $\rho/\rho_p$  is of the order of  $10^{-3}$ , the particle volume fraction can become significant only for a rather high particle loading. For low or moderate loadings the particle volume fraction can be neglected. Mathematically, a vanishing particle volume implies that  $\rho_p$  goes to infinity and  $\epsilon$  to zero in such a manner that the product  $\epsilon\rho_p$  remains finite and equal to  $\sigma_p$ .

The average distance between neighboring particles is of the order  $D/\epsilon^{1/3}$ . For particle diameters smaller than 0.1 mm, mass fractions as low as 0.03, and a density ratio  $\rho/\rho_p$  of the order of  $10^{-3}$ , the average particle spacing would be less than about 3 mm, so that both the particles and their average separations generally are small compared with the dimensions of a flow field. It then seems natural to treat the particles as a species of heavy molecules with a molecular weight that is several orders of magnitude larger than that of the gas even for particles as small as  $10^{-6}$  cm. For any mixture composition of practical interest, the number density of the particles is thus insignificant in comparison with that of the gas molecules, and the contribution of the particles to the pressure of the mixture is negligible. Therefore, the pressure of the gas-particle mixture is given by the pressure in the gas phase alone which, for a perfect gas, is

$$p = \rho R T \quad (3.6)$$

where  $R$  is the individual gas constant for the gas phase. To obtain an equation of state for the mixture, the gas density  $\rho$  in Eq. (3.6) must be expressed in terms of the mixture density which follows from Eqs. (3.1) and (3.3) as

$$\rho_m = \sigma + \sigma_p = \frac{(1-\epsilon)\rho}{1-\phi} = \frac{\epsilon\rho_p}{\phi} \quad (3.7)$$

If, then,  $\rho$  is eliminated from Eqs. (3.6) and (3.7), the equation of state for a gas-particle mixture is obtained as

$$p = \frac{\rho_m}{1 - \phi\rho_m/\rho_p} (1-\phi)RT = \frac{\rho_m}{1-\epsilon} R_m T \quad (3.8)$$

which is not the equation of state for a perfect gas since  $\rho_m$  appears both in the numerator and the denominator. The term containing  $\rho_m$  in the denominator comes from the particle volume, and the important conclusion is therefore reached that a mixture of solid particles and a perfect gas may be treated as a perfect gas only if the particle volume can be neglected. The effective gas constant of the mixture is given by

$$R_m = (1-\phi)R \quad (3.9)$$

The internal energy of the mixture is

$$E_m = (1-\phi)E + \phi E_p = (1-\phi)\epsilon_v T + \phi\epsilon T_p \quad (3.10)$$

and the enthalpy then follows from its definition as

$$H_M = E_M + \frac{p}{\rho_M} = (1-\varphi)(c_v T + \frac{p}{\rho}) + \varphi(c_p T + \frac{p}{\rho_p}) \quad (3.11)$$

because

$$\frac{1}{\rho_M} = \frac{1-\varphi}{\rho} + \frac{\varphi}{\rho_p}$$

The ratio of the two pressure terms in Eq. (3.11) is equal to  $\varepsilon/(1-\varepsilon)$  according to Eq. (3.3). The last term of the enthalpy is therefore only of the order of the particle volume fraction. Substitution of Eq. (3.6) and of the relationship

$$R = c_p - c_v$$

finally yields

$$H_M = (1-\varphi)H + \varphi H_p = (1-\varphi)c_p T + \varphi(c_p T + \varepsilon \frac{p}{\sigma_p}) \quad (3.12)$$

where  $\rho_p$  has been replaced by  $\sigma_p/\varepsilon$ , according to Eq. (3.1).

The specific heats of the equilibrium mixture at constant pressure and constant volume are defined by  $(\partial H_M/\partial T)_p$  and  $(\partial E_M/\partial T)_{\rho_M}$ . The ratio of the specific heats for the mixture,  $\gamma_M$ , therefore is related to that of the gas,  $\gamma$ , by

$$\gamma_M = \frac{c_{p,M}}{c_{v,M}} = \frac{(1-\varphi)c_p + \varphi c}{(1-\varphi)c_v + \varphi c} = \gamma \frac{1 + \xi \varphi/(1-\varphi)}{1 + \gamma \xi \varphi/(1-\varphi)} = \gamma \frac{1 + \xi \eta}{1 + \gamma \xi \eta} \quad (3.13)$$

This equation shows that the specific-heat ratio of a gas-particle mixture is always smaller than that of the gas phase. Figure 3 represents this relationship for a diatomic gas and for several values of  $\xi$  which encompass the entire range that ordinarily might be encountered; it shows the marked reductions

of the specific-heat ratio that may occur.

It is important to derive relationships that apply for isentropic (equilibrium) changes of state of a gas-particle mixture. The second law of thermodynamic yields

$$d\Delta_M = c_{v,M} \frac{dT}{T} - \frac{p}{T} \frac{d\rho_M}{\rho_M^2} = 0$$

where  $\Delta_M$  is the entropy of the mixture. This equation may be integrated if the ratio  $p/T$  is expressed in terms of  $\rho_M$  from Eq. (3.8) with the result

$$T / \left( \frac{\rho_M}{1 - \varphi \rho_M / \rho_P} \right)^{\gamma_M - 1} = \text{CONST.} \quad (3.14)$$

It is evident from Eq. (3.7) that the expression in parentheses is equal to  $\rho/(1 - \varphi)$ , and since  $\varphi$  is constant for an equilibrium mixture, one obtains

$$T / \rho^{\gamma_M - 1} = \text{CONST.} \quad (3.15)$$

and by substitution from Eq. (3.6)

$$p / \rho^{\gamma_M} = \text{CONST.} \quad (3.16)$$

Isentropic changes of state of a gas-particle mixture can therefore be computed by relationships that are analogous to those for a perfect gas, but are based on the state variables of the gas phase and the ratio of the specific heats of the mixture. This peculiar result is a consequence of the particle volume not participating in volume changes of the mixture.

The last thermodynamic property of a gas-particle mixture to be considered here is the speed of sound. As in the case of pure-gas flow, a distinction must be made between the frozen speed of sound of the mixture  $a_f$  and the equilibrium speed  $a_e$ . Frozen flow implies no viscous interaction or heat transfer between the gas and the particles so that

$$a_f^2 = a^2 = \gamma R T = \gamma \frac{p}{\rho} \quad (3.17)$$

where  $a$  is the speed of sound in the gas phase.

The equilibrium speed of sound may be derived from its definition

$$a_e^2 = \left( \frac{\partial p}{\partial \rho_e} \right)_e = \left( \frac{\partial p}{\partial \epsilon} \right)_e \left( \frac{\partial \epsilon}{\partial \rho_e} \right)_e \quad (3.18)$$

where subscripts  $e$  indicate that the derivatives must be evaluated for equilibrium (isentropic) changes of state. The first factor in Eq. (3.18) can be obtained from Eq. (3.16) and the second factor from Eqs. (3.3) and (3.7). Equations (3.6), (3.13), (3.17) and (3.18) then yield

$$\left( \frac{a_e}{a} \right)^2 = \left( \frac{a}{a_f} \right)^2 = \frac{(1-\phi) [1 + \xi \phi / (1-\phi)]}{(1-\epsilon)^2 [1 + \gamma \xi \phi / (1-\phi)]} = \frac{1 + \eta \xi}{(1-\epsilon)^2 (1+\eta) (1 + \gamma \eta \xi)} \quad (3.19)$$

All quantities on the right-hand side of the foregoing expression with the exception of  $\mathcal{E}$  depend only on the composition of the mixture, while  $\mathcal{E}$  also depends on the gas density as seen from Eq. (3.3). Since the speed of sound of the gas phase varies only with the temperature, the equilibrium speed of sound of a gas-particle mixture is a function of the temperature alone only if the particle volume can be neglected. Figure 4 shows the relationship between  $a_e/a$  and  $\phi$  for a diatomic gas and  $\rho/\rho_p = 0.01$  for three values of  $\xi$ . For the sake of clarity, only the curve for the typical value  $\xi = 1$  is plotted in its entirety, and for this case the consequences of setting  $\mathcal{E} = 0$  are also shown (broken line). Clearly, the addition of particles to a gas can lead to large reductions of the speed of sound which are only slightly affected by the value of  $\xi$ . The effect of the particle volume becomes appreciable only for large density ratios  $\rho/\rho_p$  and large particle mass fractions. As  $\phi$  approaches unity, the equilibrium speed of sound approaches zero if the particle volume is neglected and infinity (the speed of sound in the incompressible particles) if the complete formula is used. Of course, once the particle concentration becomes so large that particles are in frequent contact with one another, a solid packing is approached, and the relationships do no longer apply. Dense packing of spheres corresponds to approximately  $\mathcal{E} = 0.74$ , or  $\phi = 0.997$  in the present example. The minimum of the exact curve is reached when approximately one-half of the mixture volume is taken up by the particles (Rudinger, 1965).

Equation (3.3) indicates that the particle volume fraction is quite small except under conditions of heavy particle loading or unusually high gas densities.

For many flows, the density ratio  $\rho/\rho_p$  is of the order of 0.001, and the mass fraction of the particles is smaller than 0.5. (A typical value for a solid-propellant rocket is  $\Phi = 0.3$ .) It is therefore often permissible to neglect the particle volume and thereby avoid the complications that arise from the  $\mathcal{E}$ -terms in the equations. The assumption  $\mathcal{E} = 0$  is made in most analyses of gas-particle flow, but some aspects of a finite particle volume will be discussed in the following.

#### 4. GENERAL EQUATIONS FOR ONE-DIMENSIONAL GAS PARTICLE FLOW

Consider a flow of a gas-particle mixture through a duct of cross section  $A$  which may vary along the duct. The conditions of the gas are completely described if its velocity  $u$  and two state variables, say  $\sigma$  and  $T$ , are known as functions of position and time. Similarly, the particle conditions are described by  $u_p$ ,  $\sigma_p$  and  $T_p$ . Six simultaneous equations are therefore needed to compute the flow in a duct of prescribed shape. Often, it is convenient to introduce additional variables, such as pressure, and appropriate thermodynamic relationships, such as those derived in Section 3, then provide the needed additional equations.

To formulate the equations, the following assumptions are made. Some of these have already been discussed in the preceding sections.

1. The gas obeys the perfect-gas law, and the specific heats are constant.
2. The particles are spherical, of uniform size, and incompressible; their specific heat is constant, and the temperature is uniform within each particle.

3. The particles are uniformly distributed over the cross section of a duct, and their size and average spacing are small compared with the dimensions of the cross section of the duct.
4. The flow is treated as one-dimensional so that changes of the cross-sectional area of the duct must be sufficiently gradual. Boundary-layer effects and heat exchange with the walls are not considered. However, the viscosity and thermal conductivity of the gas enter into the calculation of particle drag and heat transfer between the gas and the particle.
5. The drag coefficient and Nusselt number are prescribed as functions of the particle Reynolds number.
6. The effect of the particles on the gas flow appears at first in the wake of the particles and is then distributed over the rest of the gas by mixing. In view of assumption No. 3, this mixing involves only a small gas volume and is therefore assumed to take place instantaneously.
7. The particles do not contribute to the pressure.
8. No external forces (such as gravity) or heat exchange affect the mixture, and no mass transfer takes place between the gas and the particles.

Derivation of the six equations to determine the flow of a gas-particle mixture in a duct of varying cross section follows the same general approach as for a pure gas (Liepmann and Roshko, 1957, Chapter 2) and will therefore not be presented in detail.

The continuity equation for the gas simply states that the net mass flux into a volume element leads to a change of the gas concentration with the element, or

$$-\frac{\partial(\sigma u A)}{\partial x} = A \frac{\partial \sigma}{\partial t} \quad (4.1)$$

An entirely analogous equation holds for the particles,

$$-\frac{\partial(\sigma_p u_p A)}{\partial x} = A \frac{\partial \sigma_p}{\partial t} \quad (4.2)$$

The momentum equation for the gas relates the acceleration of a mass element to the force that acts on it, namely, that produced by the pressure gradient and the force of the gas-particle interaction

$$\sigma \frac{Du}{Dt} = -\frac{\partial p}{\partial x} - \text{gas-particle interaction term}$$

Since the particles themselves do not exert a pressure, the corresponding equation for the particles is

$$\sigma_p \frac{D_p u_p}{Dt} = \text{gas-particle interaction term}$$

By adding these two equations, the interaction term may be eliminated once, and one obtains the momentum equation for the entire mixture as

$$\sigma \frac{Du}{Dt} + \sigma_p \frac{D_p u_p}{Dt} = -\frac{\partial p}{\partial x} \quad (4.3)$$

The momentum equation for the particles may be represented by the equation of motion for a single particle, Eq. (2.1). As discussed in connection with that equation, the viscous-drag term should be replaced by Eq. (2.4) and the pressure gradient is now given by Eq. (4.3) instead of Eq. (2.3). If these substitutions are made, and the particle volume fraction  $\mathcal{E}$  is introduced through Eq. (3.1), the equation of motion for a particle is obtained in the form

$$(1-\mathcal{E}) \frac{D_p u_p}{Dt} = C_D \frac{3}{4D} \frac{\rho}{\rho_p} |u - u_p| (u - u_p) = \Phi \quad (4.4)$$

where all other terms have been neglected as in the derivation of Eq. (2.5), because  $\rho_p$  is so much larger than  $\rho$ . It will be convenient to use  $\Phi$  as an abbreviation for the right-hand side of the equation. Comparison of Eq. (4.4) with Eq. (2.5) shows that a finite particle volume fraction introduces the factor  $(1-\mathcal{E})$  in the equation of motion of the particles.

The drag coefficient in Eq. (4.4) must be specified as some function of the particle Reynolds number as in the case of a single particle, and relationships such as those given by Eqs. (2.7a) - (2.7c) have often been used. Experimental observations indicate that the effective drag coefficient for flows of gas-particle mixtures may differ considerably from that for a single particle. Ingebo (1956) proposed the relationship

$$C_D = \frac{27}{Re^{0.84}} \quad (4.5)$$

which is also shown in Fig. 1; it lies approximately half-way between the "standard" and the Stokes drag coefficients. Wide discrepancies exist between the results obtained by different investigators. A number of these studies were reviewed by Torobin and Gauvin (1960); subsequent measurements were also made by Rudinger (1963) and Gorjup (1967), but there is as yet no general agreement as to what data should be used in a given case. This uncertainty about the drag coefficient does not affect a fundamental discussion of the relaxation phenomena, and the illustrative examples presented later in this chapter are based on Eqs. (2.7a), (2.7b) and (4.5) for which numerical results were available.

Derivation of the energy equations for a gas-particle mixture follows a reasoning analogous to that used for the momentum equations. A relationship for the entire mixture does not contain any terms that refer to the interaction between the gas and the particles. The energy equation of the mixture thus relates the net energy flux into a volume element to the rate of energy accumulation within the element, or

$$-\frac{\partial}{\partial x} \left[ \sigma u A \left( \frac{1}{2} u^2 + H \right) + \sigma_p u_p A \left( \frac{1}{2} u_p^2 + H_p \right) \right] =$$

$$A \frac{\partial}{\partial t} \left[ \sigma \left( \frac{1}{2} u^2 + E \right) + \sigma_p \left( \frac{1}{2} u_p^2 + E_p \right) \right]$$

After substitution for the internal energies and enthalpies from Eqs. (3.10) and (3.12), one obtains

$$\begin{aligned}
& - \frac{\partial}{\partial x} \left[ \sigma u A \left( \frac{1}{2} u^2 + \kappa_p T \right) + \sigma_p u_p A \left( \frac{1}{2} u_p^2 + \kappa T_p + \epsilon \frac{p}{\sigma_p} \right) \right] = \\
& A \frac{\partial}{\partial t} \left[ \sigma \left( \frac{1}{2} u^2 + \kappa T \right) + \sigma_p \left( \frac{1}{2} u_p^2 + \kappa T_p \right) \right]
\end{aligned}
\tag{4.6}$$

The energy equation for the particles may be represented by the energy balance for a single particle which follows from Eqs. (2.11) and 2.12) as

$$\frac{D_p T_p}{D t} = \frac{6 \pi \kappa N u}{\rho_p \kappa D^2} (T - T_p) = \psi
\tag{4.7}$$

where  $\psi$  is an abbreviation for the right-hand side. An appropriate relationship between the Nusselt number and the particle Reynolds number must be prescribed. Customarily, it has been assumed that the heat exchange between the gas and the particles can be described by the same Nusselt number that applies to a single particle in steady flow, and both  $Nu = 2$  (pure heat conduction) and relationships such as Eq. (2.13) (heat conduction and convection for a single particle in steady flow) have been used. It should be expected that the presence of many particles would have some effect on the effective Nusselt number, but this problem apparently has received only limited attention so far (Hoglund, 1962).

The required six equations for a gas-particle flow are thus given by Eqs. (4.1) - (4.4), (4.6) and (4.7) and appropriate assumptions for the drag coefficient and the Nusselt number. Three additional variables,  $p$ ,  $\rho$ , and  $\epsilon$ , have been introduced, and the needed extra equations are given by the equation of state for the gas, Eq. (3.6), and the relationships

between the densities and concentrations, Eqs. (3.1). It is evident that this system of equations cannot be solved analytically and that numerical solutions of specific problems are best obtained with the aid of a computer. A number of examples are presented in the following sections to illustrate the relaxation phenomena, but details of the numerical computing procedures will be omitted.

## 5. SHOCK WAVES

### a. Discontinuous Shock Front

Shock waves propagating in a duct of constant cross section represent a particularly good example of relaxation in a gas-particle mixture. If a shock wave travels through a stationary equilibrium mixture, the gas pressure and temperature undergo a practically instantaneous rise at the shock front, while the velocity decreases. Behind the shock front, the particles thus suddenly find themselves in a gas of different velocity and temperature until their subsequent interaction with the gas gradually establishes new equilibrium conditions.

In a coordinate system fixed to the shock wave, the flow is steady, and some of the equations in the preceding section then can be integrated. Let subscript zero indicate the prescribed state of the mixture upstream of the shock front and  $u_0$  the velocity with which the mixture approaches the shock. The continuity equations, Eqs. (4.1) and (4.2) then become

$$(1 - \epsilon) \rho u A = (1 - \epsilon_0) \rho_0 u_0 A = m \quad (5.1)$$

and

$$\varepsilon \rho_p u_p A = \varepsilon_o \rho_p u_o A = \eta m \quad (5.2)$$

where the concentrations of the gas and of the particles have been expressed in terms of the corresponding densities and the particle volume fraction according to Eqs. (3.1).

With the help of Eq. (2.2) with  $\partial/\partial t = 0$  (steady flow) and Eqs. (5.1) and (5.2), the momentum equation for the mixture, Eq. (4.3) can be integrated and written in the form

$$m u + \eta m u_p + A p = m (1 + \eta) u_o + A p_o \quad (5.3)$$

Integration of the energy equation, Eq. (4.6), yields

$$\frac{u^2}{2} + c_p T + \eta \left( \frac{u_p^2}{2} + c T_p + \frac{p}{\rho_p} \right) = (1 + \eta) \frac{u_o^2}{2} + (c_p + \eta c) T_o + \eta \frac{p_o}{\rho_p} \quad (5.4)$$

As pointed out in connection with Eq. (3.11), the pressure terms in this equation are of the order of the particle volume fraction.

The equation of motion and the energy balance of a particle, Eqs. (4.4) and (4.7), may be written as

$$(1 - \varepsilon) u_p \frac{du_p}{dx} = C_D \frac{3}{4D} |u - u_p| (u - u_p) \quad (5.5)$$

and

$$u_p \frac{dT_p}{dx} = \frac{6 k Nu}{\rho_p c D^2} (T - T_p) \quad (5.6)$$

In addition to Eqs. (5.1) to (5.6), the equation of state for the gas, Eq. (3.6) applies so that there are seven equations for the seven unknowns  $u, \rho, T, p, u_p, T_p$ , and  $\mathcal{E}$ .

Consider first the more important case of moderate particle loading for which the particle volume fraction can be neglected. Deletion of the terms of order  $\mathcal{E}$  in Eqs. (5.1), (5.4) and (5.5) leads to some simplification of the equations. In Eq. (5.2) the product  $\mathcal{E}\rho_p$  equals the particle concentration  $\sigma_p$  according to Eq. (3.1) and cannot be neglected. Note that the particle concentration appears only in Eq. (5.2) which thus serves to compute  $\sigma_p$  after the other unknowns have been evaluated.

During the short time in which a particle traverses the shock front, its velocity and temperature cannot be affected by viscous drag and heat transfer. The frozen state of the particles, immediately behind the shock front, is therefore given by

$$u_f = u_o \quad \text{and} \quad T_{p,f} = T_o \quad (5.7)$$

If these conditions are substituted into Eqs. (5.3) and (5.4), all terms that refer to the particles drop out, and these equations, together with Eq. (5.1), reduce to the well-known conservation equations for a shock wave in a pure gas with the solution (Liepmann and Roshko, 1957, pp. 57-60)

$$\frac{u_f}{u_o} = \frac{\rho_o}{\rho_f} = \frac{(\gamma-1) M_f^2 + 2}{(\gamma+1) M_f^2} \quad (5.8)$$

$$\frac{p_f}{p_o} = 1 + \frac{2\gamma}{\gamma+1} (M_f^2 - 1) \quad (5.9)$$

and

$$\frac{T_f}{T_o} = \frac{p_f}{p_o} \frac{\rho_o}{\rho_f} = 1 + \frac{2(\gamma-1)}{(\gamma+1)^2} \frac{\gamma M_f^2 + 1}{M_f^2} (M_f^2 - 1) \quad (5.10)$$

where the frozen shock Mach number is given by  $M_f = u_o/a_{f,o} = u_o/a_o$ , according to Eq. (3.17). The conditions in the mixture immediately behind the shock front are therefore completely determined.

The new equilibrium that is eventually established downstream of the shock front is also readily found by setting  $u = u_p = u_e$  and  $T = T_p = T_e$ . By using Eqs. (3.5), (3.13), and 3.19, it can be verified that the same shock equations are obtained as before, but this time for a gas with the thermodynamic properties of the equilibrium mixture and for an equilibrium shock Mach number  $M_e = u_o/a_{e,o}$ . The equilibrium conditions are therefore given by

$$\frac{u_e}{u_o} = \frac{\rho_o}{\rho_e} = \frac{(\gamma_e - 1) M_e^2 + 2}{(\gamma_e + 1) M_e^2} \quad (5.11)$$

$$\frac{p_e}{p_o} = 1 + \frac{2\gamma_e}{\gamma_e + 1} (M_e^2 - 1) \quad (5.12)$$

and

$$\frac{T_e}{T_o} = \frac{p_e}{p_o} \frac{\rho_o}{\rho_e} \quad (5.13)$$

Since  $a_e$  is smaller than  $a_f$ , according to Eqs. (3.17) and (3.19), it follows that  $M_e$  is greater than  $M_f$ .

The transition from frozen to equilibrium flow must be obtained by numerical integration of the equations with the initial conditions being given by the frozen flow. One method for solving the equations was suggested by Carrier (1958), who eliminated  $\alpha$  by dividing Eq. (5.6) by Eq. (5.5) and thereby obtained

$$\frac{dT_p}{du_p} = \frac{8}{\xi Pr} \frac{Nu}{C_p Re} \frac{T - T_p}{u - u_p} \approx \frac{1}{\xi} \frac{T - T_p}{u - u_p} \quad (5.14)$$

where use has been made of Eq. (2.6) and the definitions of  $\xi$  and  $Pr$ . Carrier observed that the value of the dimensionless group  $Nu / (C_p Re)$  is close to 1/12 for an appreciable range of the Reynolds number, and the approximate result given in Eq. (5.14) then follows since the Prandtl number is close to 2/3. Even with this simplification, the equations must be integrated numerically with  $u_p$  as the independent variable. Subsequently, Eq. (5.5) must also be integrated numerically to obtain the spatial distribution of the variables in the relaxation zone. It seems preferable to perform a simultaneous numerical integration of Eqs. (5.5) and (5.6) for prescribed drag coefficients and Nusselt numbers. Details of this procedure will be omitted, but a few results are given here. Such data for different mixtures and shock strengths, and for various drag coefficients and Nusselt numbers have been published by Kliegel (1963), Marble (1963a), Kriebel (1964), Rudinger (1964), Varma and Chopra (1967), and others.

A typical shock transition is shown in Fig. 5 for 10- $\mu$  glass spheres suspended in air for  $\eta = 0.2$ ; this mixture has the properties  $\gamma = 1.40$ ,  $\gamma_m = 1.30$ , and  $\xi = 1.125$ . The calculations are based on Ingebo's drag coefficient, Eq. (4.5), on a Nusselt number given by Eq. (2.13), and on a shock strength  $M_f = 1.50$ , corresponding to  $M_e = 1.70$ . Equilibrium conditions are shown in the figure, and it can be seen that the relaxation zone extends over a considerable distance. As discussed after Eq. (2.10), the time required by a particle to traverse the relaxation zone is roughly proportional to the square of the particle size. Furthermore, since the initial deviation of the gas velocity from the particle velocity is an indication of the shock strength, Eq. (5.5) shows that equilibrium is approached faster for stronger shock waves. Kriebel (1964) observed that the length of the relaxation zone also increases with decreasing shock strength. Wide variations in the length of the relaxation zone may therefore be encountered.

It is interesting to note that the gas velocity decreases behind the shock although the particle velocity is higher than the gas velocity. This decrease is a consequence of the simultaneous effects of viscous drag and gas-particle heat transfer; it is closely related to the well-known increase of a subsonic flow velocity in an adiabatic duct with wall friction. The general validity of this behavior may be established by forming the ratio  $u_f / u_e$  from Eqs. (5.8) and (5.11), replacing  $M_f$  by  $u_o / a_o$  and  $M_e$  by  $u_o / a_{e,o}$ , and then substituting Eqs. (3.13) and (3.19) for  $\gamma_m$  and  $a_{e,o}$ ; the resulting expression for  $u_f / u_e$  is readily proven to be greater than unity for all possible conditions. Similarly, Eqs. (5.9) and

(5.12) may be used to show that  $p_e$  is always greater than  $p_f$ .

Since the particle velocity in the relaxation zone is always larger than the gas velocity, the decrease of  $u_p$  is monotonic, as seen from Eq. (5.5), but under some extreme conditions, the derivative  $(du/dx)_{x=0}$  may become positive so that the gas velocity then goes through a maximum before decreasing to its equilibrium value. This situation cannot occur as long as  $M_f^2 < 2\gamma/(\gamma-1)$ , and even for stronger shocks, it is necessary (Rudinger, 1964) that the two conditions

$$\gamma G < 1$$

and

$$M_f^2 > \frac{2\gamma + (\gamma-1)G}{(\gamma-1)(1-\gamma G)}$$

be satisfied simultaneously, where

$$G = \frac{g}{P_r} \left( \frac{Nu}{C_D Re} \right)_{x=0}$$

If both the gas velocity and the particle velocity decrease monotonically, then Eq. (5.3) indicates that the pressure increases monotonically. Similar conclusions do not hold for the gas temperature. Equation (5.6) shows that the particle temperature increases monotonically from  $T_{p,f} = T_o$  to  $T_e$  since  $T_f$  is higher than  $T_{p,f}$ , but  $T_f$  may be higher or lower than  $T_e$ , and the transition may not even be monotonic (Rudinger, 1964, Varma and Chopra, 1967, see also the discussion of Fig. 7).

The uncertainty of the drag coefficient and Nusselt number for gas-particle flows is discussed in Section 4. It is therefore important to see

what effect these parameters have on the relaxation zone. Figure 6 shows the gas pressure and the particle velocity for the same conditions as for Fig. 5, but with different assumptions for  $C_D$  and  $Nu$ , and Fig. 7 shows the corresponding gas and particle temperatures. It is quite evident that the assumption for the drag coefficient has a significant effect on the particle velocity and the gas pressure, while the assumption for the Nusselt number has only a minor effect. \* In contrast, the gas and particle temperatures are significantly affected by the assumption made for the Nusselt number and only to a lesser extent by that for the drag coefficient. In this example,  $T_g$  is greater than  $T_p$ , and the transition is monotonic or exhibits a maximum or minimum. Figure 5 indicates that the gas velocity decreases only slightly in the relaxation zone, and the variations caused by different assumptions for the drag coefficient and Nusselt number are not shown since they amount to not more than a few percent.

Modifications of the relaxation zone result if the particle loading becomes high enough that the particle volume should not be neglected. During the time in which a particle crosses the shock front, the pressure difference across the shock acts on the particle while it traverses the front and slightly changes its velocity (Wright, 1951). Equation (2.1) then simplifies to the form

$$\rho_p u_p \frac{du_p}{dt} = - \frac{dp}{dx} \quad (5.15)$$

---

\*This observation forms the basis for studies to determine the effective drag coefficient experimentally (Rudinger, 1963).

which yields the relationship between particle velocity and pressure difference across the shock front

$$u_{p,f}^2 = u_o^2 - 2 \frac{p_f - p_o}{\rho_p}$$

Since the deviation of  $u_f$  from  $u_o$  is small, this equation may be linearized to yield

$$u_{p,f} = u_o - \frac{p_f - p_o}{\rho_p u_o} = u_o - \frac{p_f - p_o}{\eta m} A \epsilon_o \quad (5.16)$$

where Eq. (5.2) has been used to substitute for  $\rho_p u_o$ . The frozen particle volume fraction then follows from Eq. (5.2) which shows that

$$\epsilon_f = \epsilon_o \quad (5.17)$$

to the same accuracy as  $u_{p,f}$ . The frozen particle temperature  $T_{p,f}$  is equal to  $T_o$  as before. These results, substituted into Eqs. (5.1), (5.3) and (5.4), again yield the conservation equations for a pure gas, so that the frozen conditions in the gas are given by Eqs. (5.8) to (5.10), accurate to the first order of the particle volume fraction.

The effects of the particle volume on the equilibrium conditions are more significant. If  $u = u_p = u_e$  and  $T = T_p = T_e$  are substituted into Eqs. (5.1) to (5.4), the system of equations can be solved by successive elimination of unknowns with the result (Rudinger, 1965)

$$\frac{u_e}{u_o} = \frac{(\gamma_n - 1)M_e^2 + 2 + 2\mathcal{E}_o(M_e^2 - 1)}{(\gamma_n + 1)M_e^2} \quad (5.18)$$

$$\mathcal{E}_e = \mathcal{E}_o \frac{u_o}{u_e} \quad (5.19)$$

$$\frac{\rho_e}{\rho_o} = \frac{(1 - \mathcal{E}_o) u_o}{(1 - \mathcal{E}_e) u_e} \quad (5.20)$$

$$\begin{aligned} \frac{p_e}{p_o} &= 1 + \frac{(1 - \mathcal{E}_o) \gamma (1 + \eta) (u_o - u_e) u_o}{a_o^2} = \\ &= 1 + \frac{2\gamma_n}{\gamma_n + 1} (M_e^2 - 1) \end{aligned} \quad (5.21)$$

and

$$\frac{T_e}{T_o} = \frac{p_e}{p_o} \frac{\rho_o}{\rho_e} \quad (5.22)$$

Since  $M_f/M_e = a_e/a_f$ , it follows that the square of this ratio is given directly by Eq. (3.19). The particle volume therefore affects the results both indirectly through modification of the equilibrium Mach number and directly through additional terms in the equations.

The effects of the particle volume on the equilibrium velocity is shown in Fig. 8 as a function of the dimensionless velocity upstream of the shock wave -- the frozen Mach number -- for several values of  $\eta$  and  $\mathcal{E}_o$ , and for  $\gamma = 1.4$  and  $\xi = 1$ . Clearly, the effect is significant for  $\mathcal{E}_o = 0.01$  and can be quite large for  $\mathcal{E}_o$  greater than 0.05. For example, for  $\eta = 10$  and  $u_o/a_o = 1.5$ , the correct value of  $u_e/a_o$  is about 0.079, while

a value of only 0.064 would be obtained if the particle volume were neglected. It follows from Eq. (3.5) that the foregoing example corresponds to a ratio of  $\rho_s/\rho_r$  of only  $10^{-3}$ .

The effect of the particle volume on the equilibrium pressure is fairly small as seen in Fig. 9. For the example given in the foregoing, the exact value of  $p_s/p_r$  is 32.6 compared with a value of 33.4 if the particle volume is neglected. The curves in Figs. 8 and 9 are extended to frozen shock Mach numbers below unity. This case is discussed in the next section.

The transition from frozen to equilibrium conditions must be determined by numerical integration of Eqs. (5.5) and (5.6) with simultaneous consideration of Eqs. (5.1) to (5.4) and (3.6), as in the case for negligible particle volume. Apparently, the only calculations of this kind were performed by Varma and Chopra (1967) for particle volume fractions of 0.05 and 0.1 and loading ratios of 1 and 5. Their results indicate transition zones that appear similar to those shown in Figs. 5 to 7 except that the gas velocity goes through a shallow minimum before approaching its equilibrium value when  $\xi$  is not equal to zero. However, these authors disregarded the  $\xi$ -term in Eq. (5.5), and the influence of this term has not yet been evaluated.

#### b) Dispersed Shock Waves

Shock transition from the initial to the final equilibrium conditions is possible only if the mixture approaches the shock wave with a velocity that exceeds the equilibrium speed of sound. On the other hand, a discontinuous shock front in the gas phase requires that the velocity exceeds the frozen speed of sound, that is, the speed of sound in the gas phase.

As discussed after Eq. (3.19), the frozen speed of sound is greater than the equilibrium speed so that there exists a velocity range for which a shock transition is possible but a discontinuous shock front is not. Within this range  $a_f > u_0 > a_e$ , the transition takes the form of a dispersed shock wave. Analogous dispersed transitions occur in relaxing pure gases for sufficiently weak waves (Griffith and Kenny, 1957, or the chapter on shock waves by E. Becker in this volume).

Transition with a discontinuous shock front changes to a dispersed wave occurred at that limiting value of the equilibrium Mach number at which the frozen Mach number becomes unity, or when  $M_{e,lim} = a_f / a_e$ . These values can be obtained from Eq. (3.19) and are plotted in Fig. 10 as a function of the particle mass fraction for three values of  $\xi$ . The calculations are based on  $\gamma = 1.4$ , and the small effect of the particle volume has been neglected. Clearly, the particle mass fraction is of major importance, while the value of  $\xi$  has a comparatively small effect. It is evident that dispersed shocks of substantial strength are possible compared with similar shocks in relaxing gases which are extremely weak. For example, Griffith and Kenny (1957) indicate that the limiting shock Mach number for a dispersed shock in carbon dioxide is only 1.042.

Numerical evaluation of the flow in the transition zone is based on the same equations as for the case of a discontinuous shock front except that a small deviation from the initial equilibrium must be assumed to provide starting conditions for the calculations. Kriebel (1964) assumed perturbations of the gas velocity and temperature produced by a weak hypothetical compression wave and obtained the perturbations of the other variables

compatible with the equations. Rudinger (1964) linearized the equations and obtained a set of compatible initial perturbations in terms of an arbitrary perturbation of the gas velocity. Figure 11 represents the results for a typical relaxation zone computed for the same conditions as for Fig. 5 except that now  $M_f = 0.95$ , corresponding to  $M_e = 1.08$ . Comparison of Figs. 5 and 11 also shows how much the length of the relaxation zone is increased for the weaker shock, as discussed in Section 5a.

The effect of a finite particle volume on the equilibrium conditions, indicated by Eqs. (5.18) to (5.22), is shown in Figs. 8 and 9. The curves are extended to values of  $M_f$  below unity until the limit  $M_e = 1$  is reached. This limit is shown in Fig. 8; in Fig. 9 it corresponds to  $p_e/p_o = 1$  according to Eq. (5.21).

## 6. NOZZLE FLOW

Nozzle flows of gas-particle mixtures may be significantly affected by relaxation effects. In a typical problem, the flow is steady, and the shape of the nozzle is prescribed. The continuity equations, Eqs. (4.1) and (4.2), again reduce to Eqs. (5.1) and (5.2), except that the cross-sectional area of the duct now is not constant but a prescribed function  $A(x)$ . Because of the variable area, Eq. (4.3), combined with the continuity equations, cannot be integrated, so that the momentum equation takes the form

$$\frac{du}{d\chi} + \eta \frac{du_p}{d\chi} + \frac{A}{m} \frac{dp}{d\chi} = 0 \quad (6.1)$$

The energy equation, Eq. (4.6), becomes

$$u \frac{du}{d\chi} + c_p \frac{dT}{d\chi} + \eta \left( u_p \frac{du_p}{d\chi} + c \frac{dT_p}{d\chi} + \frac{1}{\rho_p} \frac{dp}{d\chi} \right) = 0 \quad (6.2a)$$

but sometimes it is more convenient to use the integrated form

$$\frac{u^2}{2} + c_p T + \eta \left( \frac{1}{2} u_p^2 + c T_p + \frac{p}{\rho_p} \right) = \text{const} \quad (6.2b)$$

where the constant is determined by prescribed inlet or reservoir conditions. In addition, Eqs. (3.6), (4.4), and (4.7) apply, so that a complete set of seven equations for the seven variables  $u, T, p, \rho, u_p, T_p$  and  $\mathcal{E}$  is established. If the particle volume can be neglected, a simplified system is obtained since the  $\mathcal{E}$ -terms in Eqs. (5.1) and (4.4) and the pressure terms in Eq. (6.2) can be omitted; Eq. (5.2) then becomes an equation for the particle concentration  $\sigma_p = \mathcal{E} \rho_p$ , as in the case of shock waves.

Equations that are identical or substantially equivalent to those given here have been published by Kliegel (1960 and 1963), Soo (1961), Bailey, Nielson, Serra and Zupnik (1961), Glauz (1962), Rannie (1962), Duban and Nicolas (1963), Marble (1963b), Hassan (1964), Hultberg and Soo (1965), and others.

One approach to solving the system of equations is to prescribe the flow at the nozzle inlet and integrate the equations numerically. A difficulty must then be expected when the nozzle throat is reached because the prescribed mass flow may not be able to pass through the throat, or in the case of a converging-diverging nozzle, the flow may decelerate instead of accelerate downstream of the throat. Since the maximum flow rate that can just pass through a given throat depends on the relaxation processes, the correct mass flow cannot be accurately prescribed beforehand, and various computational techniques have been used to overcome this difficulty. They all are based on some iteration in which the flow rate or the throat area are varied until the flow can just pass through the throat. Once a solution for the flow has been obtained, any data of interest may be derived. For example, the specific impulse of the jet emerging from a nozzle, defined as thrust/weight flow rate, has been evaluated for various nozzle shapes to find optimum configurations (Marble, 1963b, or Duban and Nicolas, 1963).

Often, it is desired to obtain a better general understanding of the flow properties rather than finding numerical answers to specific problems. Other techniques then might be preferred. One of these is based on the assumption that deviations from equilibrium are small. If one sets  $\mathcal{E} = 0$ ,  $u = u_p$  and  $T = T_p$ , the equations reduce to the form that applies to one-dimensional nozzle flow of a perfect gas with the thermodynamic properties of a gas-particle mixture outlined in Section 2. Small deviations from this flow may then be analyzed by linearizing the equations. This approach has been used, for instance, by Rannie (1962) and Marble (1963b) who obtained analytical relationships between the deviations of the variables from their equilibrium values.

Another approach, which is not limited to small deviations from equilibrium, is based on an inverse method. For qualitative studies, one may assume Stokes drag, Eq. (2.7e), and  $Nu = 2$ . Furthermore, the particle volume may be neglected for moderate loading ratios. From Eqs. (5.5), (5.6), (2.10) and (2.15) it follows then that the particle velocity and temperature obey the relationships

$$u_p \frac{du_p}{dz} = \frac{1}{\tau_v} (u - u_p) \quad (6.3)$$

and

$$u_p \frac{dT_p}{dz} = \frac{1}{\tau_T} (T - T_p) \quad (6.4)$$

It is immediately apparent that the gas velocity follows directly from Eq. (6.3) if the particle velocity is prescribed by some function of  $z$ . The other variables may then be obtained by proper combination of the equations of the system. In particular, the cross-sectional area is now one of the unknowns, so that the shape of the nozzle depends on the initial assumptions made for  $u_p$ .

This method has been used by Gilbert, Davis, and Altman (1955) to evaluate the effects of the velocity lag of the particles on the specific impulse of a nozzle. These authors made the assumption that the particle velocity increases linearly with the distance traveled. More general studies were performed by Kliegel (1960, 1963) who assumed the particle velocity to be directly proportional to the distance. Subsequently, Hassan (1964) considered particle velocities proportional to the square root of the distance.

The following discussion is based on Kliegel's approach which yields particularly convenient results. If  $u_p$  is assumed to be proportional to  $\lambda$ , Eq. (6.3) shows that then

$$\frac{u_p}{u} = K \quad (6.5)$$

where  $K$  is a constant. The lag of the particle temperature may be indicated by the ratio

$$\frac{T_\lambda - T_p}{T_\lambda - T} = L \quad (6.6)$$

where subscript  $\lambda$  denotes the reservoir conditions of the flow. Kliegel showed that the parameter  $L$  is related to  $K$  by

$$L = \left(1 + 3 Pr \xi \frac{1-K}{K}\right)^{-1} \quad (6.7)$$

and is therefore also constant; he termed nozzles with these properties "constant-fractional-lag nozzles". The interesting property of such nozzles is that the flow equations reduce to the form that applies to the flow of a perfect gas which has an apparent specific-heat ratio  $\bar{\gamma}$  and in which the Mach number is given by  $\bar{M}$ ; these quantities are determined by

$$\bar{\gamma} = 1 + (\gamma - 1) \frac{B}{C} \quad (6.8)$$

and

$$\bar{M}^2 = CM^2 \quad (6.9)$$

where  $M = u/a$ ,

$$B = \frac{1 + \eta K^2}{1 + \eta \xi L} \quad (6.10)$$

and

$$C = 1 + \eta \{K[(1-K)\bar{\gamma} + K] + (\bar{\gamma}-1)\xi LB\} \quad (6.11)$$

The solution of the flow equations is thus given by the well-known relationships

$$\frac{T_r}{T} = 1 + \frac{\bar{\gamma}-1}{2} \bar{M}^2 \quad (6.12)$$

$$\frac{\rho_r}{\rho} = \left(\frac{T_r}{T}\right)^{\frac{1}{\bar{\gamma}-1}} \quad (6.13)$$

$$\frac{p_r}{p} = \left(\frac{T_r}{T}\right)^{\frac{\bar{\gamma}}{\bar{\gamma}-1}} \quad (6.14)$$

$$\frac{A}{A_*} = \frac{1}{M} \left[ \frac{2}{\bar{\gamma}+1} \left( 1 + \frac{\bar{\gamma}-1}{2} \bar{M}^2 \right) \right]^{\frac{\bar{\gamma}+1}{2(\bar{\gamma}-1)}} \quad (6.15)$$

$$\frac{u}{u_{max}} = \left[ \frac{(\bar{\gamma}-1) \bar{M}^2}{2 + (\bar{\gamma}-1) \bar{M}^2} \right]^{\frac{1}{2}} \quad (6.16)$$

where an asterisk indicates throat conditions;  $u_{max}$  is the velocity reached for an infinite expansion and is given by

$$u_{max}^2 = \frac{2 c_p T_a}{B} \quad (6.17)$$

Integration of Eq. (6.3) yields the distribution of the gas velocity along the nozzle as

$$u = \frac{1-K}{K} \frac{x}{\tau_v} \quad (6.18)$$

The flow is therefore completely determined since the constants  $\tau_v$ ,  $B$ ,  $C$ , and  $u_{max}$  follow from the properties of the gas-particle mixture and the selected value of  $K$ . It is readily verified with the aid of Eqs. (3.13) and (3.19) that Eqs. (6.8) and (6.9) reduce to  $\bar{\gamma} = \gamma_m$  and  $\bar{M} = M_e$  for equilibrium flow for which  $K = L = 1$ .

The maximum flow rate through the nozzle throat is obtained by setting  $\bar{M} = 1$  in Eqs. (6.13), and (6.15) to (6.18) and is given by

$$(m + m_p)_{max} = m_{max} (1 + \eta) = (1 + \eta) \left( \frac{2}{\bar{\gamma} + 1} \right)^{\frac{1}{\bar{\gamma} - 1}} \left( \frac{\bar{\gamma} - 1}{\bar{\gamma} + 1} \right)^{1/2} p_a \tau_{max} A^* \quad (6.19)$$

A few of Kliegel's (1963) numerical results are indicated by Figs. 12 to 14. Figure 12 shows how  $\bar{\gamma}$  increases with increasing deviation from equilibrium flow for two loading ratios of a typical metalized rocket propellant, and Fig. 13 represents the corresponding maximum flow rates divided by the flow rates for equilibrium. It can be seen that the maximum flow rate increases significantly with increasing lags.

Combination of Eqs. (6. 15), (6. 16) and (6. 18) yields an expression for the nozzle profile

$$\left(\frac{A}{A_*}\right)^{1/2} = \left(\frac{\bar{\gamma}-1}{\bar{\gamma}+1}\right)^{1/4} \frac{1}{\bar{Z}^{1/2}} \left[ \frac{2}{(\bar{\gamma}+1)(1-\bar{Z}^2)} \right]^{\frac{1}{2(\bar{\gamma}-1)}} \quad (6.20)$$

where

$$\bar{Z} = \frac{1-K}{K^2} \frac{\chi}{\tau_v u_{max}} \quad (6.21)$$

is a dimensionless coordinate. The throat is located at  $\bar{Z}_*$  where the derivative of  $A$  with respect to  $\bar{Z}$  vanishes, and Eq. (6. 20) yields  $\bar{Z}_* = (\bar{\gamma}-1)/(\bar{\gamma}+1)$ . Figure 14 shows the nozzle profile for  $\bar{\gamma} = 1.2$  as a function of the dimensionless distance from the throat  $\bar{Z} - \bar{Z}_*$ . This plot indicates that a constant-fractional-lag nozzle may be a satisfactory approximation of actual nozzles, at least in the vicinity of the throat.

The author, in an investigation to be published, has extended Kliegel's concept of the fractional-lag nozzle to particle loadings so high that the particle volume had to be considered. The numerical analysis then becomes considerably more complicated, but it is possible to make an approximation which leads to convenient results. Computer solutions for such flows indicate that the gas and particle temperatures remain substantially constant throughout the nozzle. This observation is plausible because isothermal flow implies a specific-heat ratio of unity and this value is rapidly approached with increasing loading ratios. For example, Eq. (3. 13) yields  $\bar{\gamma}_M = 1.027$  for  $\bar{\gamma} = 1.4$ ,  $\xi = 1$  and  $\eta = 10$  and still smaller

values for higher loading ratios. It seems therefore reasonable to assume  $T = T_p = T_r = \text{const.}$  Two unknowns are thus eliminated and with them the energy equation, Eq. (6.2), and the heat balance of a particle, Eq. (6.4). The remaining Eqs. (5.1), (5.2), (6.1) and (3.6) may be combined and integrated with the result

$$u^2 = u_o^2 + \frac{2RT_n}{1+\eta K} \left[ \ln \frac{p_o}{p} + \frac{\epsilon_o}{1-\epsilon_o} \left( 1 - \frac{p}{p_o} \right) \right] \quad (6.22)$$

where subscript zero denotes prescribed conditions at the nozzle inlet.

Other variables then follow from

$$\frac{\epsilon}{1-\epsilon} = \frac{\epsilon_o}{1-\epsilon_o} \frac{p}{p_o} \quad (6.23)$$

and

$$\frac{A}{A_o} = \frac{u_o p_o (1-\epsilon_o)}{u p (1-\epsilon)} \quad (6.24)$$

The equation of motion of the particles, Eq. (6.3), multiplied by  $(1-\epsilon)$  as in Eq. (5.5), may be used to find the longitudinal area variations by numerical integration.

The nozzle throat is reached when the derivative of  $A$  with respect to  $p$  vanishes. With this condition, Eqs. (6.22) to (6.24) yield

$$2 \ln \frac{p}{p_o} - \left( \frac{\epsilon_o}{1-\epsilon_o} \frac{p_o}{p} \right)^2 - 4 \frac{\epsilon_o}{1-\epsilon_o} \frac{p_o}{p} = 1 - \frac{1+\eta K}{RT_n} u_o^2 - 2 \frac{\epsilon_o}{1-\epsilon_o} \quad (6.25)$$

The throat velocity and particle volume follow from Eqs. (6.22) and (6.23).

The foregoing results may be compared with "exact" data obtained by numerical integration of the equations without assuming isothermal flow. Such a comparison is shown in Fig. 15 where the ratio of the approximate to the "exact" results is plotted as a function of the initial particle volume fraction or the loading ratio for  $\gamma = 1.4$ ,  $\xi = 1.0$ ,  $\rho_n / \rho_p = 5 \times 10^{-4}$ ,  $u_* = 0.1 a_{e,n}$ , and  $K = 0.6$ . It is evident that the errors introduced by the assumption of isothermal flow are below 2% if the loading ratio exceeds approximately 10. If the  $\mathcal{E}$ -terms in the foregoing equations are neglected, extremely simple relationships are obtained, and the corresponding results are shown in Fig. 15 as the broken lines. In this case the errors remain below 2% as long as the loading ratio does not exceed about 100. Thus, there exists a range of the loading ratio, roughly between 10 and 100, within which both isothermal flow and negligible particle volume may be assumed. The deviations from the "exact" results become larger for lower loading ratios because the flow is no longer sufficiently isothermal, and for higher loading ratios because the particle volume is no longer sufficiently small. However, a much wider range of the loading ratio may be treated in the simple manner indicated if a lower accuracy is acceptable.

## 7. NONSTEADY FLOW

The flows in the illustrative examples given in the preceding sections are all steady. A brief discussion of more general nonsteady flows is given in this section. The equations which describe such flows have already been stated in Section 4 as Eqs. (4.1) to (4.4), (4.6), (4.7) and (3.6), and the only simplification introduced in the following will be the assumption of negligible particle volume.

The particle conditions are therefore given by

$$\frac{D_p u_p}{Dt} = \Phi \quad (7.1)$$

$$\frac{D_p T_p}{Dt} = \Psi \quad (7.2)$$

where  $\Phi$  and  $\Psi$  are abbreviations for the right-hand side of Eqs. (4.4) and (4.7), and

$$\frac{D_p \sigma_p}{Dt} = - \sigma_p \left( \frac{\partial u_p}{\partial x} + \frac{u_p}{A} \frac{\partial A}{\partial x} \right) \quad (7.3)$$

For the gas, it seems preferable to describe the conditions in terms of its velocity  $u$ , speed of sound  $a$ , related to  $T$ ,  $p$  and  $\rho$  by Eq. (3.17), and the entropy given by the thermodynamic relationship

$$\frac{s-s_0}{R} = \frac{2\gamma}{\gamma-1} \ln \frac{a}{a_0} - \ln \frac{p}{p_0}$$

where subscript zero denotes a suitable reference state.

The continuity equation then becomes

$$\frac{2}{\gamma-1} \frac{Da}{Dt} + a \frac{\partial u}{\partial x} = - \frac{au}{A} \frac{\partial A}{\partial x} - \frac{a}{R} \frac{Ds}{Dt} \quad (7.4)$$

and the momentum equation, after substitution from Eq. (7.1), takes the form

$$\frac{Du}{Dt} + \frac{2}{\gamma-1} a \frac{\partial a}{\partial x} = \frac{a^2}{\gamma R} \frac{\partial s}{\partial x} - \frac{\sigma_p}{\rho} \Phi \quad (7.5)$$

The energy equation is most conveniently combined with Eqs. (7.1), (7.2) and (7.5) and may then be written as

$$\frac{Ds}{Dt} = \frac{\sigma_p}{\rho} \frac{\partial R}{\partial x} \left[ (u - u_p) \Phi - \kappa \psi \right] \quad (7.6)$$

By setting  $\sigma_p = 0$  in the last three equations, the equations for non-steady flow of a pure gas are obtained, and these are usually solved numerically by means of the method of characteristics (Courant and Friedrichs, 1948, Rudinger, 1955, or Fox, 1962). An extension to gas-particle flows was first provided by Chu and Parlange (1962) who linearized the equations under the assumption that deviations from equilibrium are small. A more general approach may be taken by deriving the characteristic relationships for the complete equations. Rudinger and Chang (1964) treated the unknown gas and particle conditions as one set of unknowns, while Migdal and Agosta (1967) considered the particle terms in the equations as sources or sinks of drag and heat transfer in a pure gas flow. There seems to be little practical difference between these two points of view.

The foregoing system of six simultaneous partial differential equations has six characteristic velocities which are given by

$$\frac{dx}{dt} = u \pm a \quad (7.7)$$

$$\frac{dx}{dt} = u \quad (7.8)$$

and

$$\frac{dx}{dt} = u_p \quad (7.9)$$

which must be counted threefold. The triple degeneracy indicated by the last equation was explained by Sauerwein and Fendell (1965) as a consequence of neglecting the partial pressure of the particles. In a more rigorous treatment, the speed of sound in the particle phase would be given by  $a_p^2 = \gamma_p p_p / \sigma_p$  where  $\gamma_p$  is the ratio of specific heats and  $p_p$  the pressure of the particle phase; Eq. (7.9) would then split to yield the three velocities  $u_p$  and  $u_p \pm a_p$ . Equation (7.9) is then a consequence of setting  $p_p = 0$ .

Flow changes along the characteristics are described by the compatibility equations which take the form

$$\frac{d^+P}{dt} = -\frac{au}{A} \frac{\partial A}{\partial x} + \frac{a}{\gamma R} \frac{d^+s}{dt} + \frac{\gamma-1}{\gamma R} a \frac{D_s}{Dt} - \frac{\sigma_p}{\rho} \Phi \quad (7.10)$$

$$\frac{d^-Q}{dt} = -\frac{au}{A} \frac{\partial A}{\partial x} + \frac{a}{\gamma R} \frac{d^-s}{dt} + \frac{\gamma-1}{\gamma R} a \frac{D_s}{Dt} + \frac{\sigma_p}{\rho} \Phi \quad (7.11)$$

for the characteristics given by Eq. (7.7), where

$$\frac{d^+}{d\tau} = \frac{\partial}{\partial t} + (u \pm a) \frac{\partial}{\partial x} \quad (7.12)$$

represents derivatives along these characteristics, and  $P$  and  $Q$  are the well-known Riemann variables of nonsteady gas flow defined by

$$P = \frac{2}{\gamma-1} a + u \quad (7.13)$$

and

$$Q = \frac{2}{\gamma-1} a - u \quad (7.14)$$

The derivatives along the other characteristics are indicated by Eqs. (7.1) to (7.3) and (7.6). Equation (7.3) may be used for numerical work, although it is not a true compatibility equation. Sauerwein and Fendell (1965) pointed out that compatibility equations should contain only derivatives in the characteristic directions and showed that the present result is a consequence of the already mentioned degeneracy.

A numerical evaluation of a given problem may now be set up for prescribed initial and boundary conditions in the same manner as for nonsteady flow of a pure gas. As an illustrative example (Rudinger and Chang, 1964) consider a semi-infinite tube of constant cross section filled with a mixture of 30-  $\mu$  glass spheres in atmospheric air at a loading ratio of 0.3. A piston at the end of the tube is impulsively accelerated from rest to such a speed that the velocity  $u_0$  of the resultant shock wave initially equals  $1.3 a_0$ , where  $a_0$  is the initial speed of sound in the gas. In this example, Stokes

drag, Eq. (2.7a), and  $Nu = 2$  have been assumed to characterize the particle drag and heat transfer. The gas flowing behind the shock wave gradually accelerates the particles and, in this process, its own velocity is affected. Waves signaling these changes propagate upstream and downstream. When the upstream-traveling waves reach the piston, they are reflected so that the gas velocity at the piston remains equal to the piston velocity. Both the waves originally traveling downstream and those reflected at the piston eventually overtake the shock wave and in merging with it reduce its strength. These wave processes are indicated in Fig. 16 which shows the piston path, the shock path and the trajectories of a typical particle and of a gas element. Particles that initially are close to the piston collide with it before reaching equilibrium with the gas and are assumed to remain attached to the piston surface. As a result of the changing shock strength, the shock path is not a straight line, but this change is better seen in Fig. 17 where the shock velocity is plotted as a function of the distance traveled by the shock wave. The ultimate steady velocity reached by the shock wave is also shown in the figure; it may be computed directly on the basis of equilibrium flow and the shock relationships given in Section 5a. The shock velocity decreases from its initial value of  $1.3 a_0$  to an equilibrium value of  $1.124 a_0$  over a distance of several meters. By comparison, Fig. 16 indicates that the particles should reach their final velocity after only 20 to 30 cm, or about one order of magnitude faster. The large difference between particle and shock relaxation may be significant for investigations of the particle motion since it may then be permissible to neglect changes of shock strength during the relaxation time of the particles.

## 8. CONCLUDING REMARKS

The relationships presented in this chapter describe thermodynamic properties, shock waves, steady nozzle flows and general nonsteady, one-dimensional flow of gas-particle mixtures. Relaxation effects arise because viscous drag and heat transfer cannot adjust the particle velocity and temperature fast enough to maintain equilibrium conditions. These interactions also lead to modifications of the gas flow. Ordinarily, other relaxation effects need not be considered because they are either so fast that instantaneous establishment of equilibrium may be assumed or so slow that frozen conditions represent a good approximation for a significant part of the flow. The volume occupied by the particles frequently can be neglected with resultant simplifications of the analysis, but appreciable consequences of the particle volume may appear if the particle loading is sufficiently high.

A number of typical examples clearly demonstrate the importance of velocity and temperature relaxation. The rates of these processes are approximately proportional to the inverse square of the particle diameter but do not depend on the dimensions of the flow system. Therefore, changes in the size of the system produce approximately similar flows only if the particle diameter can be scaled in proportion to the square root of the duct dimensions.

## 9. LIST OF SYMBOLS

$a$	speed of sound
$A$	cross-sectional area of duct
$B$	constant, Eq. (6.10)
$c$	specific heat of particle material
$c_p, c_v$	specific heats of the gas at constant pressure and at constant volume
$C$	constant, Eq. (6.11)
$C_D$	drag coefficient
$D$	particle diameter
$E$	internal energy
$H$	enthalpy
$h$	heat-transfer coefficient
$k$	thermal conductivity
$K$	velocity ratio in a constant-fractional-lag nozzle, Eq. (6.5)
$L$	temperature ratio in a constant-fractional-lag nozzle, Eq. (6.6)
$M$	shock or flow Mach number
$\bar{M}$	effective Mach number in a constant-fractional-lag nozzle
$m$	mass flow rate of gas phase
$Nu$	Nusselt number
$Pr$	Prandtl number
$p$	pressure
$P, Q$	characteristic variables, Eqs. (7.13) and (7.14)

$R$	gas constant
$Re$	Reynolds number
$s$	entropy
$T$	temperature
$u$	velocity
$x$	coordinate along duct
$Z$	dimensionless form of $x$
$\gamma$	ratio of specific heats
$\bar{\gamma}$	effective ratio of specific heats in a constant-fractional-lag nozzle
$\epsilon$	volume fraction of the particles
$\eta$	mass flow ratio
$\kappa$	thermal diffusivity
$\mu$	viscosity
$\xi$	$= c/c_p$
$\rho$	density
$\sigma$	concentration
$\tau_v$	relaxation time for velocity
$\tau_T$	relaxation time for temperature
$\tau_i$	temperature equalization time for a particle
$\phi$	mass fraction of particles
$\Phi$	right-hand side of Eq. (4.4)
$\Psi$	right-hand side of Eq. (4.7)

### Subscripts

$0$	initial or reference conditions
$f$	frozen flow
$e$	equilibrium flow
$r$	reservoir conditions
$M$	equilibrium mixture
$p$	particle conditions if different from gas conditions
$*$	conditions at nozzle throat

### Derivatives

$$\frac{D}{Dt}, \frac{D_p}{Dt} \quad \text{Eq. (2.2)}$$

$$\frac{\delta^t}{\delta t} \quad \text{Eq. (7.12)}$$

## 10. REFERENCES

- Bailey, W.S., Nielson, E.N., Serra, R.A. & Zupnik, T.F., 1961, Gas Particle Flow in an Axisymmetric Nozzle. ARS Journal 31, 793-798.
- Carlson, D.J. & Hoglund, R.F., 1964, Particle Drag and Heat Transfer in Rocket Nozzles. AIAA Journal 2, 1980-1984.
- Carrier, G.F., 1958, Shock Waves in a Dusty Gas. J. Fluid Mech. 4, 376-382.
- Carslaw, H.S. & Jaeger, J.C., 1959, Conduction of Heat in Solids. 2nd Ed., Oxford University Press, London, p.234.
- Chu, B.T. & Parlange, J.Y., June 1962, A Microscopic Theory of Two-Phase Flow With Mass, Momentum and Energy Exchange. Brown University Technical Report No. 4, (AD-277-975).
- Courant, R. & Friedrichs, K.O., 1948, Supersonic Flow and Shock Waves. Interscience Publishers, Inc., New York.
- Crowe, C.T., 1967, Drag Coefficient of Particles in a Rocket Nozzle. AIAA Journal 5, 1021-1022.
- Duban, P. & Nicolas, J., 1963, Influence de la Présence de Particules Solides Sur l'Écoulement Dans une Tuyère. La Recherche Aéronautique 92, 17-29.
- Fox, L., 1962, Numerical Solution of Ordinary and Partial Differential Equations. Addison-Wesley Publishing Company, Inc., Reading, Massachusetts.
- Fuchs, N.A., 1964, The Mechanics of Aerosols. Macmillan Co., New York.
- Gilbert, M., Davis, L. & Altman, D., 1955, Velocity Lag of Particles in Linearly Accelerated Combustion Gases. Jet Propulsion 25, 26-30.
- Glauz, R.D., 1962, Combined Subsonic-Supersonic Gas-Particle Flow. ARS Journal 32, 773-775.
- Gordon, G.D., 1959, Mechanism and Speed of Breakup of Drops. J. Applied Physics 30, 1759-1761.
- Gorjup, M., 1967, Calibration of a Micrometeoroid Impact Gauge. Institute for Aerospace Studies, University of Toronto, UTIAS Technical Note No. 97.

- Griffith, W. C., & Kenny, A., 1957, On Fully-Dispersed Shock Waves in Carbon Dioxide. *J. Fluid Mechanics* 3, 286-288.
- Hassan, H. A., 1964, Exact Solutions of Gas-Particle Nozzle Flows. *AIAA Journal* 2, 395-396.
- Hinze, J. O., 1959, Turbulence. McGraw-Hill Book Company, New York, Chapters 5-7.
- Hoenig, S. A., 1957, Acceleration of Dust Particles by Shock Waves. *Journal of Applied Physics* 28, 1218-1219.
- Hoglund, R. F., 1962, Recent Advances in Gas-Particle Nozzle Flows. *ARS Journal* 32, 662-671.
- Hultberg, J. A. & Soo, S. L., 1965, Two-Phase Flow Through a Nozzle. *Astronautica Acta* II, 207-216.
- Ingebo, R. D., 1956, Drag Coefficients for Droplets and Solid Spheres in Clouds Accelerated in Air Streams, NACA TN 3762.
- Kliegel, J. R., January 25-27, 1960, One-Dimensional Flow of a Gas-Particle System. Paper No. 60-5 presented at the 28th Annual Meeting of the Institute of Aeronautical Sciences, New York.
- Kliegel, J. R., 1963, Gas-Particle Nozzle Flows. Ninth Symposium (International) on Combustion, Academic Press, New York, pp. 811-826.
- Knudsen, J. G. & Katz, D. L., 1958, Fluid Mechanics and Heat Transfer. McGraw-Hill Book Company, New York, p. 511.
- Kriebel, A. R., 1964, Analysis of Normal Shock Waves in Particle Laden Gas. *Trans. ASME Series D (Journal of Basic Engineering)* 86, 655-664.
- Liepmann, H. W., & Roshko, A., 1957, Elements of Gasdynamics. John Wiley & Sons, Inc., New York.
- Marble, F. E., 1963a, Dynamics of a Gas Containing Small Solid Particles. Combustion and Propulsion (5th AGARDograph Colloquium), Pergamon Press, Oxford, pp. 175-213.
- Marble, F. E., 1963b, Nozzle Contours for Minimum Particle-Lag Loss. *AIAA Journal* 1, 2793-2801.
- Migdal, D. & Agosta, V. D., 1967, A Source Flow Model for Continuum Gas-Particle Flow. *Trans. ASME Series E, (Journal of Applied Mechanics)* 34, 860-865.
- Putnam, A., 1961, Integratable Form of Droplet Drag Coefficient. *ARS Journal* 31, 1467-1468.

Rannie, W.D., 1962, Perturbation Analysis of One-Dimensional Heterogeneous Flow in Rocket Nozzles. Detonation and Two-Phase Flow. Penner, S.S., & Williams, F.A., Editors, Academic Press, New York pp. 117-144.

Rudinger, G., 1955, Wave Diagrams for Nonsteady Flow in Ducts. D. Van Nostrand Publishing Company, Inc., Princeton, New Jersey (to be republished by Dover Publications, Inc., New York).

Rudinger, G., 1963, Experiments on Shock Relaxation in Particle Suspensions in a Gas and Preliminary Determination of Particle Drag Coefficients. Multiphase Symposium (Lipstein, N.J., Editor), ASME, New York, pp. 55-61. (Later experimental data to be published).

Rudinger, G., 1964, Some Properties of Shock Relaxation in Gas Flows Carrying Small Particles. Physics of Fluids 7, 658-663.

Rudinger, G., & Chang, A., 1964, Analysis of Nonsteady Two-Phase Flow. Physics of Fluids 7, 1747-1754.

Rudinger, G., 1965, Some Effects of Finite Particle Volume on the Dynamics of Gas-Particle Mixtures. AIAA Journal 3, 1217-1222.

Rudinger, G., (to be published), Gas-Particle Flow in Convergent Nozzles at High Loading Ratios.

Sauerwein, H. & Fendell, F.E., 1965, Method of Characteristics in Two-Phase Flow. Physics of Fluids 8, 1564-1565.

Schaaf, S.A. & Chambré, P.L., 1958, Flow of Rarefied Gases In High Speed Aerodynamics and Jet Propulsion, (Emmons, H., Editor). Princeton University Press, Princeton, New Jersey, Vol. III, (Fundamentals of Gas Dynamics), Section H.

Schlichting, H., 1955, Boundary Layer Theory. McGraw-Hill Book Co., Inc., New York, p. 16.

Simmons, F.S. & Spadaro, F.G., 1965, Thermal Lag of Solid Carbon in Rocket Nozzle Flow. Pyrodynamics 2, 177-189.

Soo, S.L., 1961, Gas Dynamic Processes Involving Suspended Solids. A.I.Ch.E. Journal 7, 384-391.

Torobin, L.B. & Gauvin, W.H., 1960, Fundamental Aspects of Solids-Gas Flow, Part V: The Effects of Fluid Turbulence on the Particle Drag Coefficient. Canad. J. of Chemical Engineering, 38, 189-200.

Varma, T.D. & Chopra, N.K., 1967, Analysis of Normal Shock Waves in a Gas-Particle Mixture. ZAMP 18, 650-660.

Willis, D. R., 1966, Sphere Drag at High Knudsen Number and Low Mach Number. *Physics of Fluids* 9, 2522-2524.

Wright, F. H., 1951, The Particle-Track Method of Tracing Fluid Streamlines. Jet Propulsion Lab., California Inst. of Technology, Progr. Rept. No. 3-23.

## FIGURE CAPTIONS

- Fig. 1 Drag coefficient for particles.
- Fig. 2 Nusselt number for particles.
- Fig. 3 Ratio of the specific heats of a gas-particle mixture for a diatomic gas and various relative specific heats
- $$\bar{\gamma} = c/c_p \quad (\text{after Rudinger 1965}).$$
- Fig. 4 Equilibrium speed of sound for a gas-particle mixture (after Rudinger, 1965).
- Fig. 5 Typical relaxation zone behind a shock front. Computed for a mixture of  $10\text{-}\mu$  glass spheres and air at standard temperature and pressure at a mass-flow ratio  $\eta = 0.2$  and a shock velocity  $u_s/a_s = M_f = 1.50$ , corresponding to  $\bar{\gamma} = 1.125$ ,  $\gamma_M = 1.30$ ,  $a_{s,p}/a_s = 0.88$ , and  $M_e = 1.70$ . The calculations are based on Ingebo's drag, and steady-flow heat transfer (after Rudinger, 1964a).

Fig. 6                      Effect of different assumptions for particle drag and heat transfer on the pressure and the particle velocity for the same mixture and shock strength as for Fig. 5 (after Rudinger, 1964).

<u>Drag Coefficient</u>	<u>Nusselt Number</u>	
	<u>Steady Flow</u>	<u>Nu = 2</u>
"Standard"	A	B
Ingebo	C	D
Tokes	E	F

Fig. 7                      Effect of different assumptions for particle drag and heat transfer on the gas and particle temperatures for the same conditions as for Fig. 6.

Fig. 8                      Effect of particle volume on the equilibrium velocity behind a shock front (after Rudinger, 1965).

Fig. 9                      Effect of particle volume on the equilibrium pressure behind a shock front (after Rudinger, 1965).

Fig. 10                    Limiting (minimum) shock Mach number for a discontinuous shock front.

Fig. 11                    Typical dispersed shock wave. Computed for the same mixture as for Fig. 5 but for  $M_f = 0.95$ , corresponding to  $M_e = 1.08$ .

- Fig. 12                      Apparent ratio of the specific heats for a constant-fractional-lag nozzle for a typical metalized rocket propellant (after Kliegel, 1963).
- Fig. 13                      Effect of velocity lag of the particles on the total mass flow for a constant-fractional-lag nozzle and a typical metalized rocket propellant (after Kliegel, 1963).
- Fig. 14                      Profile of a constant-fractional-lag nozzle for  $\bar{\gamma} = 1.20$  (after Kliegel, 1963).
- Fig. 15                      Comparison of throat conditions for a constant-fractional-lag nozzle obtained by the "exact" and approximate equations.
- Fig. 16                      Piston impulsively accelerated in a mixture of 10- $\mu$  diameter glass particles in air at a loading ratio  $\eta = 0.3$ . The initial shock velocity is  $1.3 a_s$ , and the calculations are based on Stokes drag and  $Nu = 2$  (after Rudinger and Chang, 1964).
- Fig. 17                      Shock velocity ahead of impulsively accelerated piston for example of Fig. 16 (after Rudinger and Chang, 1964).

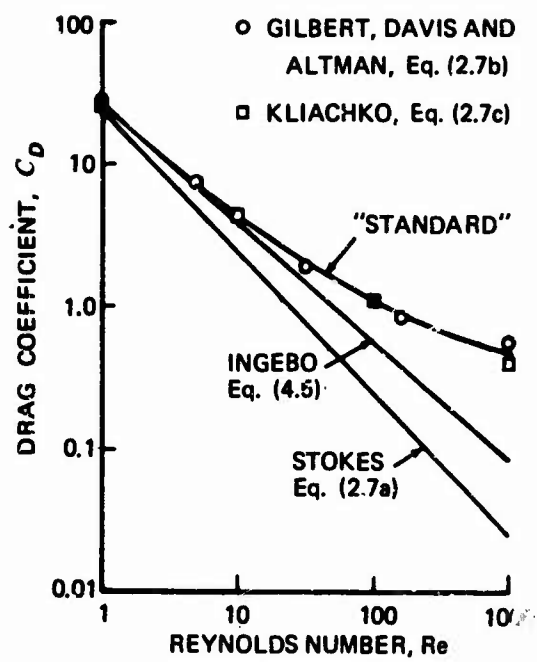


Figure 1 DRAG COEFFICIENT FOR PARTICLES.

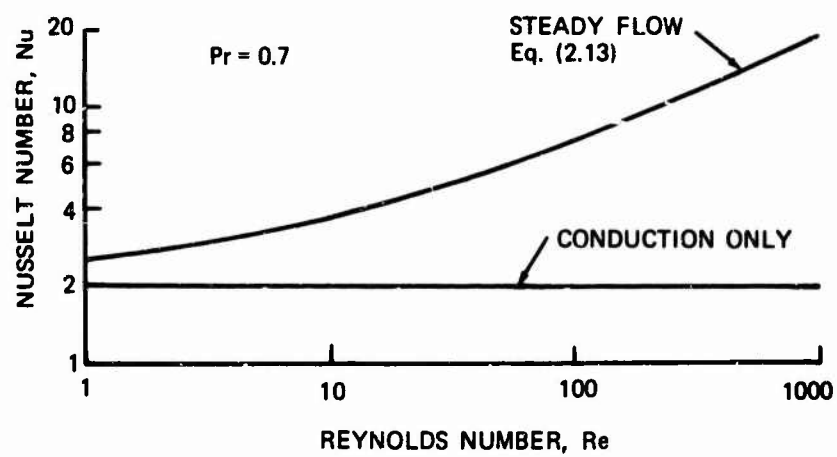


Figure 2 NUSSELT NUMBER FOR PARTICLES.

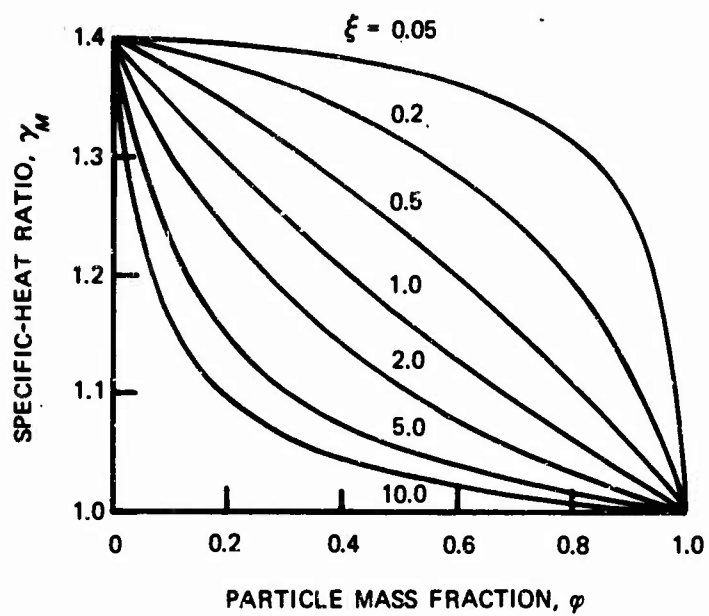


Figure 3 RATIO OF THE SPECIFIC HEATS OF A GAS-PARTICLE MIXTURE FOR A DIATOMIC GAS AND VARIOUS RELATIVE SPECIFIC HEATS  $\xi = c/c_p$  (AFTER RUDINGER 1965).

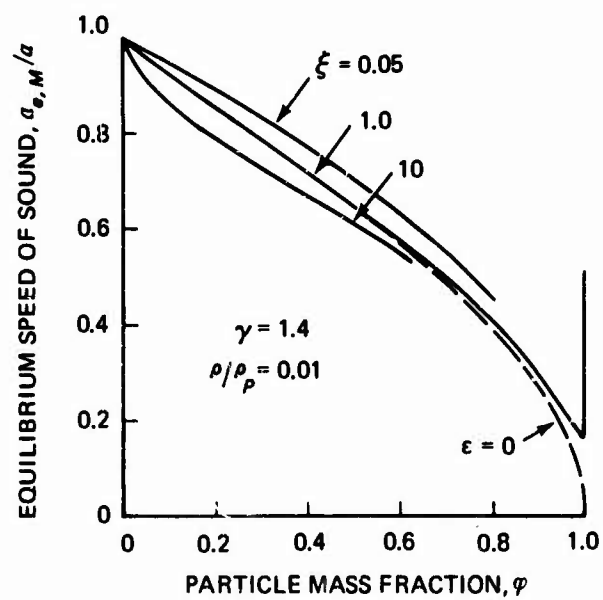


Figure 4 EQUILIBRIUM SPEED OF SOUND FOR A GAS-PARTICLE MIXTURE (AFTER RUDINGER, 1965).

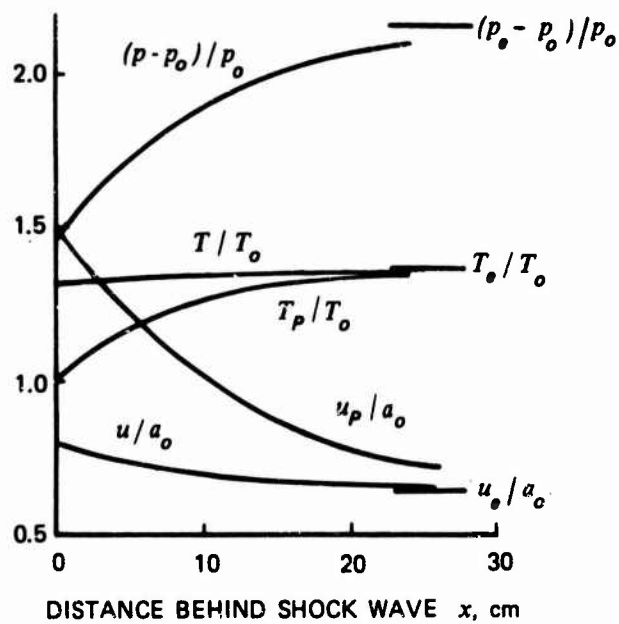


Figure 5 TYPICAL RELAXATION ZONE BEHIND A SHOCK FRONT. COMPUTED FOR A MIXTURE OF  $10\mu$  GLASS SPHERES AND AIR AT STANDARD TEMPERATURE AND PRESSURE AT A MASS-FLOW RATIO  $\eta = 0.2$  AND A SHOCK VELOCITY  $u_o/a_o = M_f = 1.50$  CORRESPONDING TO  $\xi = 1.125$ ,  $\gamma_M = 1.30$ ,  $a_{e,o}/a_o = 0.88$  AND  $M_e = 1.70$ . THE CALCULATIONS ARE BASED ON INGEBO'S DRAG AND STEADY-FLOW HEAT TRANSFER (AFTER RUDINGER, 1964a).

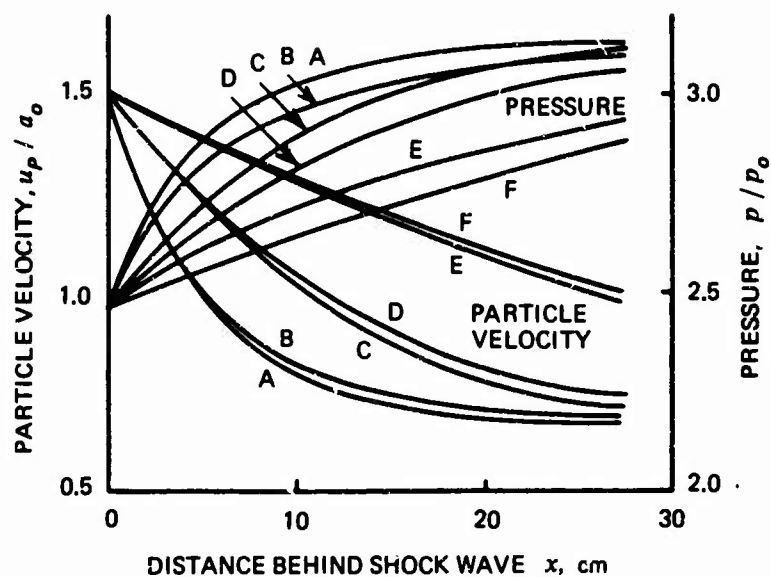


Figure 6 EFFECT OF DIFFERENT ASSUMPTIONS FOR PARTICLE DRAG AND HEAT TRANSFER ON THE PRESSURE AND THE PARTICLE VELOCITY FOR THE SAME MIXTURE AND SHOCK STRENGTH AS FOR FIGURE 5 (AFTER RUDINGER, 1964).

<u>DRAG COEFFICIENT</u>	<u>NUSSELT NUMBER</u>	
	<u>STEADY FLOW</u>	<u>NU = 2</u>
"STANDARD"	A	B
INGEBO	C	D
STOKES	E	F

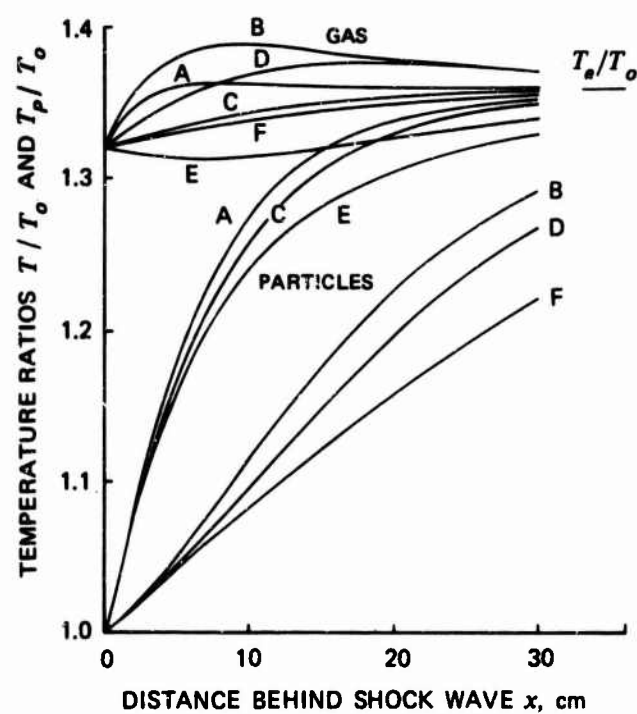


Figure 7 EFFECT OF DIFFERENT ASSUMPTIONS FOR PARTICLE DRAG AND HEAT TRANSFER ON THE GAS AND PARTICLE TEMPERATURES FOR THE SAME CONDITIONS AS FOR FIGURE 6.

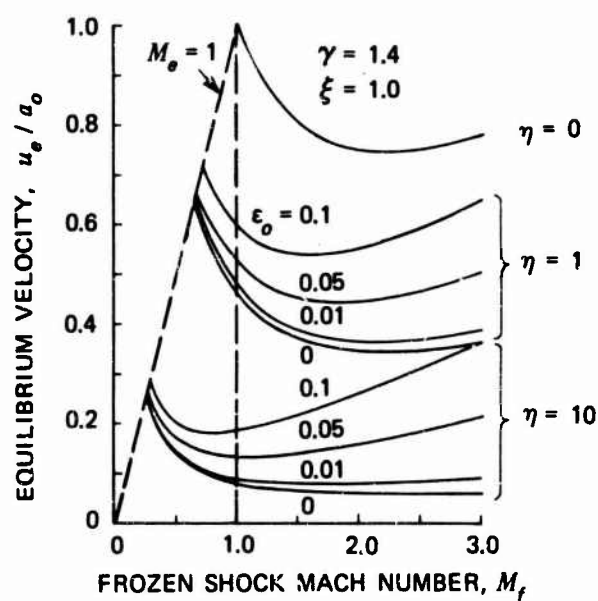


Figure 8 EFFECT OF PARTICLE VOLUME ON THE EQUILIBRIUM VELOCITY BEHIND A SHOCK FRONT (AFTER RUDINGER, 1965).

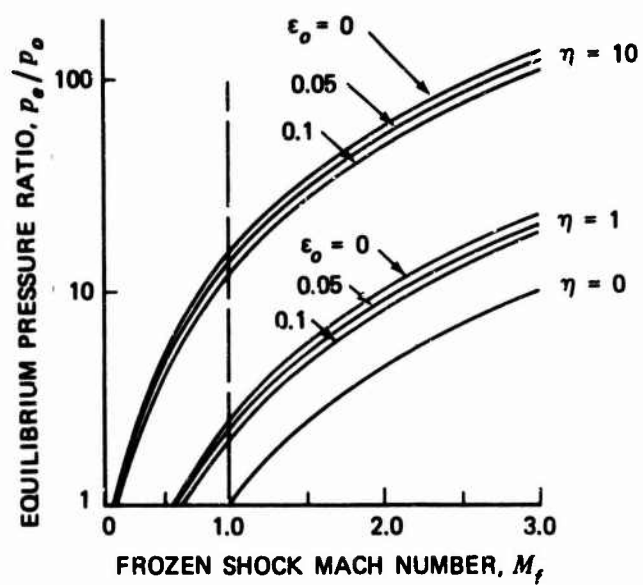


Figure 9 EFFECT OF PARTICLE VOLUME ON THE EQUILIBRIUM PRESSURE BEHIND A SHOCK FRONT (AFTER RUDINGER, 1965).

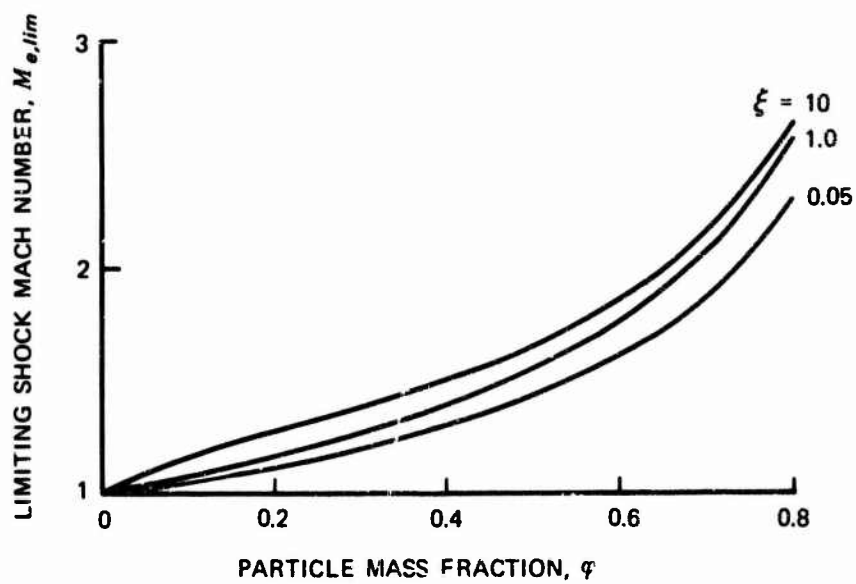


Figure 10 LIMITING (MINIMUM) SHOCK MACH NUMBER FOR A DISCONTINUOUS SHOCK FRONT.

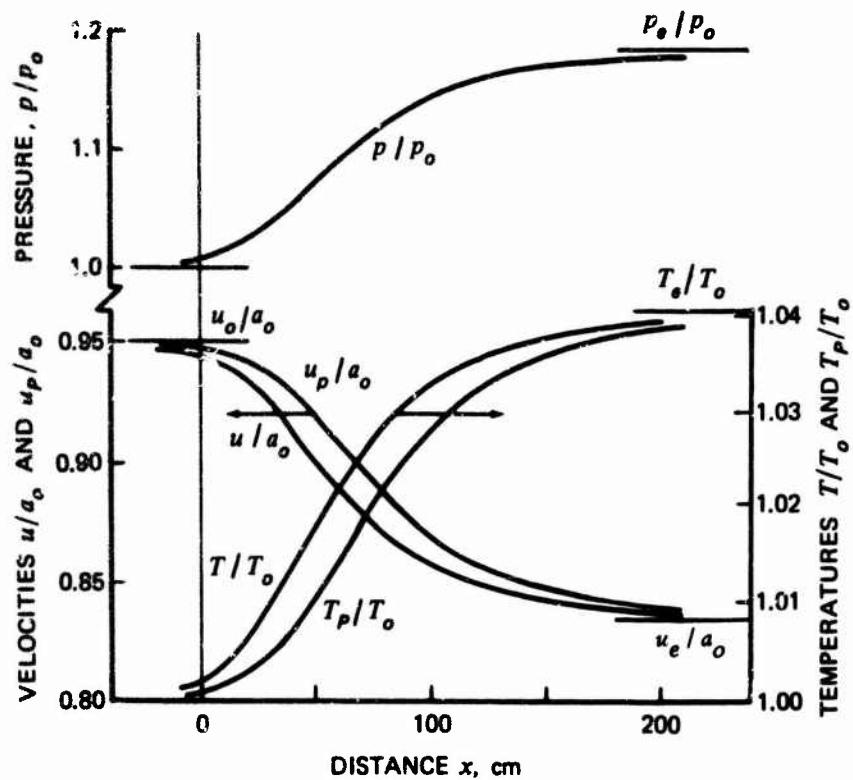


Figure 11 TYPICAL DISPERSED SHOCK WAVE. COMPUTED FOR THE SAME MIXTURE AS FOR FIGURE 5 BUT FOR  $M_f = 0.95$ , CORRESPONDING TO  $M_o = 1.08$ .

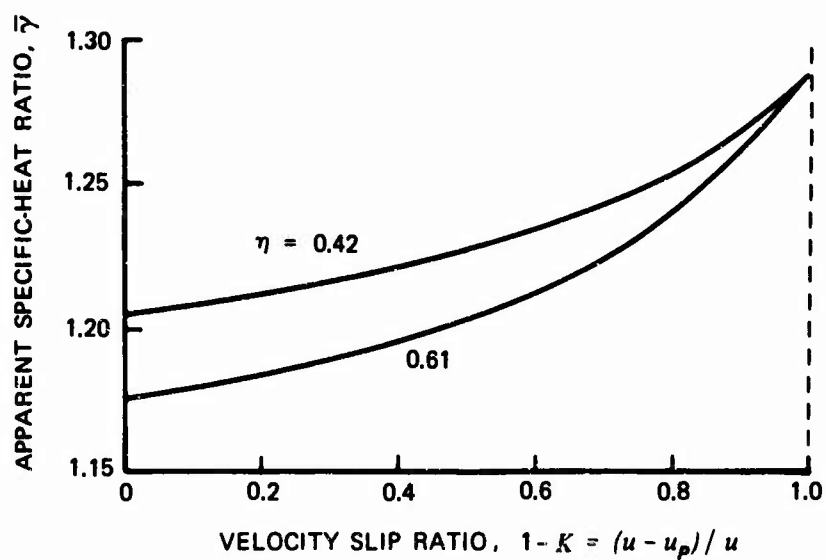


Figure 12 APPARENT RATIO OF THE SPECIFIC HEATS FOR A CONSTANT-FRACTIONAL-LAG NOZZLE FOR A TYPICAL METALIZED ROCKET PROPELLANT (AFTER KLIEGEL, 1963).

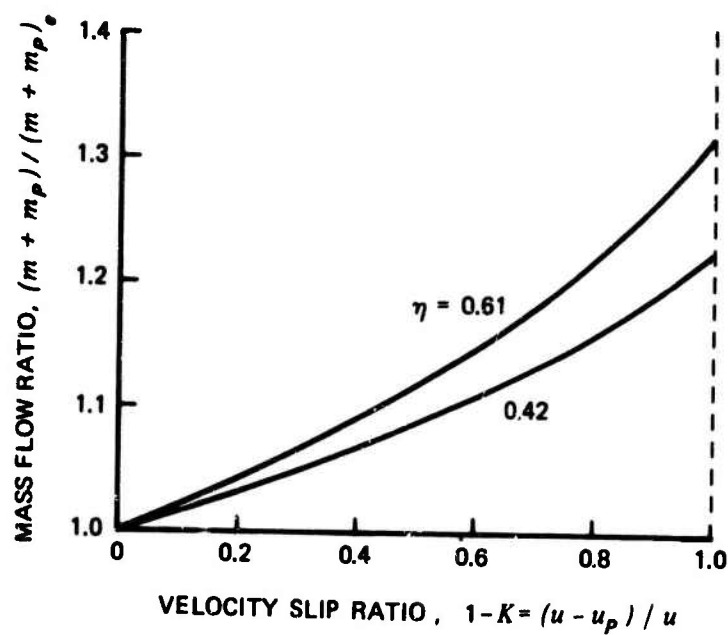


Figure 13 EFFECT OF VELOCITY LAG OF THE PARTICLES ON THE TOTAL MASS FLOW FOR A CONSTANT-FRACTIONAL-LAG NOZZLE AND A TYPICAL METALIZED ROCKET PRO-  
 PELLANT (AFTER KLIEGEL, 1963).

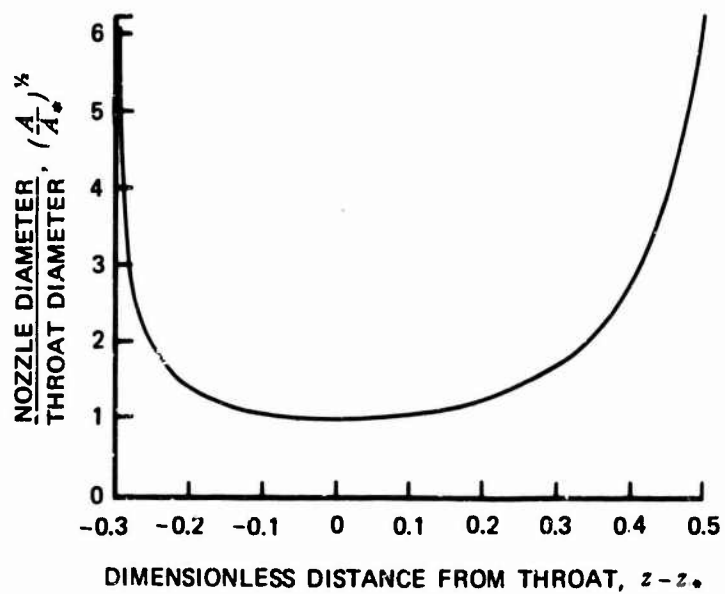


Figure 14 PROFILE OF A CONSTANT-FRACTIONAL-LAG NOZZLE  
FOR  $\bar{\gamma} = 1.20$  (AFTER KLIEGEL, 1963).

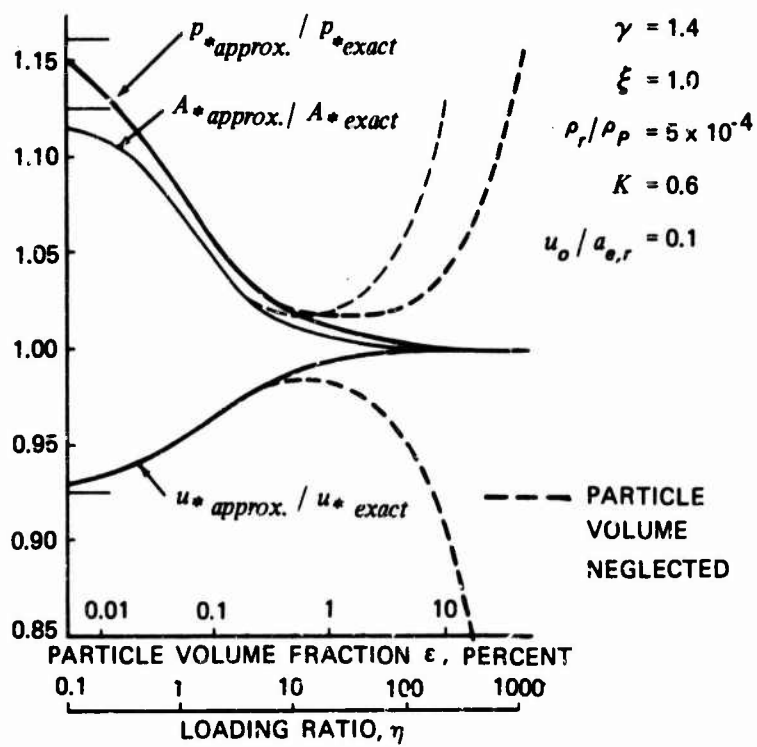


Figure 15 COMPARISON OF THROAT CONDITIONS FOR A CONSTANT-FRACTIONAL-LAG NOZZLE OBTAINED BY THE "EXACT" AND APPROXIMATE EQUATIONS.

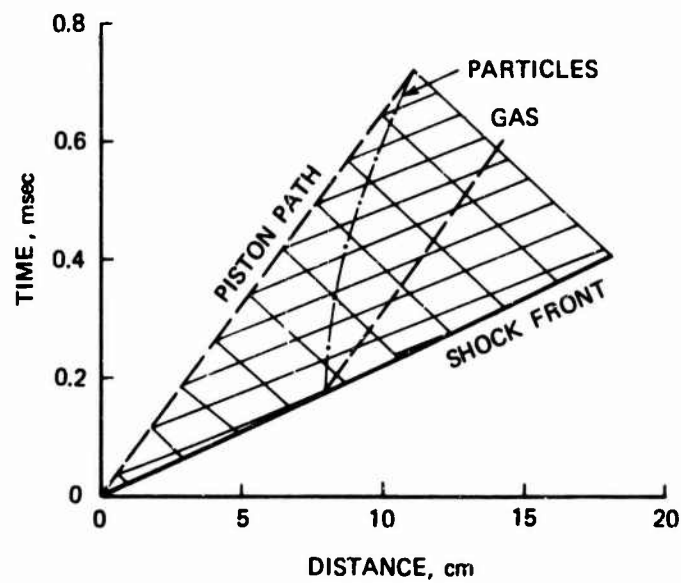


Figure 16 PISTON IMPULSIVELY ACCELERATED IN A MIXTURE OF  $10\mu$  DIAMETER GLASS PARTICLES IN AIR AT A LOADING RATIO  $\eta = 0.3$ . THE INITIAL SHOCK VELOCITY IS  $1.3a_0$ , AND THE CALCULATIONS ARE BASED ON STOKES DRAG AND  $Nu = 2$  (AFTER RUDINGER AND CHANG, 1964).

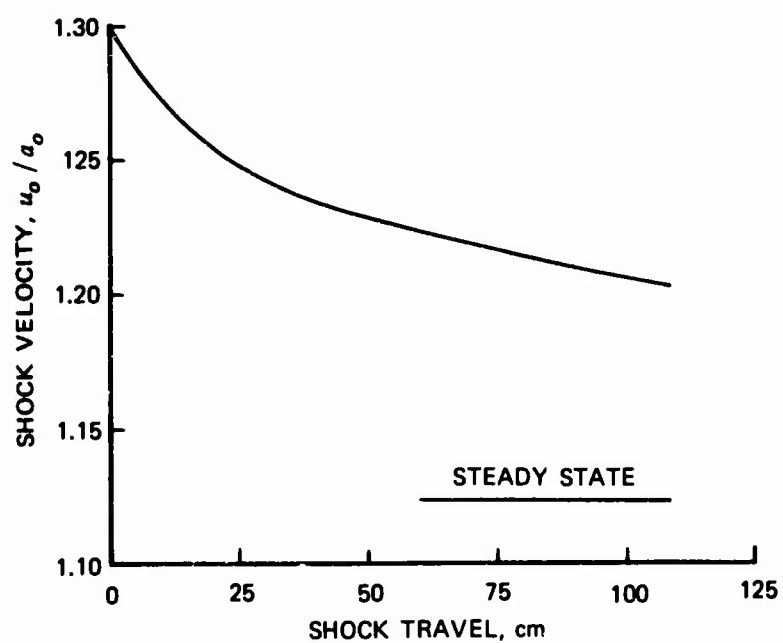


Figure 17 SHOCK VELOCITY AHEAD OF IMPULSIVELY ACCELERATED PISTON FOR EXAMPLE OF FIGURE 16 (AFTER RUDINGER AND CHANG, 1964).

UNCLASSIFIED

Security Classification

## DOCUMENT CONTROL DATA - R &amp; D

(Security classification of title, body of abstract and indexing annotation must be entered when the overall report is classified)

1. ORIGINATING ACTIVITY (Corporate author) Project SQUID Jet Propulsion Center, School of Mechanical Eng'g Purdue University, Lafayette, Indiana 47907		2a. REPORT SECURITY CLASSIFICATION UNCLASSIFIED	
		2b. GROUP N/A	
3. REPORT TITLE  RELAXATION IN GAS-PARTICLE FLOW			
4. DESCRIPTIVE NOTES (Type of report and inclusive dates) N/A			
5. AUTHOR(S) (First name, middle initial, last name) George Rudinger			
6. REPORT DATE July 1968		7a. TOTAL NO. OF PAGES 81	7b. NO. OF REFS 46
8a. CONTRACT OR GRANT NO. N00014-67-A-0226-0005		9a. ORIGINATOR'S REPORT NUMBER(S) CAL-96-PU	
b. PROJECT NO. NR-098-038		9b. OTHER REPORT NO(S) (Any other numbers that may be assigned this report)	
c.			
d.			
10. DISTRIBUTION STATEMENT  Qualified requesters may obtain copies of this report from DDC.			
11. SUPPLEMENTARY NOTES N/A		12. SPONSORING MILITARY ACTIVITY Office of Naval Research Power Branch, Code 429 Dept. of the Navy, Washington, D.C. 20360	
13. ABSTRACT Flow of gas-particle mixtures may exhibit significant relaxation effects if the particle velocity and temperature cannot follow rapid changes in the flow conditions. These relaxation phenomena are first demonstrated in a discussion of viscous drag and heat transfer for a single particle which has no effect on the gas flow. If there are enough particles to make up a significant fraction of the mass of the mixture, the thermodynamic properties of the mixture may differ considerably from those of the gas alone, and a number of these properties are derived. Equations for one-dimensional flow of uniform mixtures are applied to shock waves, steady nozzle flows, and general nonsteady flows to illustrate the relaxation processes. For low and moderate particle concentration, the volume occupied by the particles can often be neglected. Since this assumption may not be adequate for high concentrations, some effects of a finite particle volume are also discussed.			

DD FORM 1473  
1 NOV 65UNCLASSIFIED  
Security Classification

